NASA TECHNICAL NOTE

NASA TN D-4329

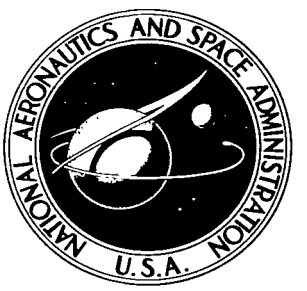

NASA TN D-4329

MEASUREMENTS OF GROUND EFFECT ON A LOW-ASPECT-RATIO OGEE-WING AIRPLANE MODEL AND CALCULATIONS OF LANDING-FLARE TRAJECTORIES

by Vernard E. Lockwood and W. Pelham Phillips

Langley Research Center
Langley Station, Hampton, Va.

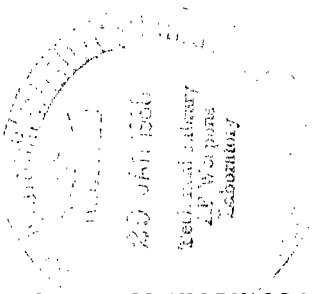

NATIONAL AERONAUTICS AND SPACE ADMINISTRATION • WASHINGTON, D. C. • JANUARY 1968

MEASUREMENTS OF GROUND EFFECT ON A LOW-ASPECT-RATIO OGEE-WING AIRPLANE MODEL AND CALCULATIONS OF LANDING-FLARE TRAJECTORIES

By Vernard E. Lockwood and W. Pelham Phillips

Langley Research Center
Langley Station, Hampton, Va.

NATIONAL AERONAUTICS AND SPACE ADMINISTRATION

For sale by the Clearinghouse for Federal Scientific and Technical Information
Springfield, Virginia 22151 – CFSTI price $3.00

MEASUREMENTS OF GROUND EFFECT ON A LOW-ASPECT-RATIO OGEE-WING AIRPLANE MODEL AND CALCULATIONS OF LANDING-FLARE TRAJECTORIES

By Vernard E. Lockwood and W. Pelham Phillips
Langley Research Center

SUMMARY

An investigation has been made to determine the ground effect on a 0.15-scale model of a fighter-type airplane having an ogee-wing planform. The characteristics in close proximity to the ground were determined by utilizing the moving-belt facility of the Langley 300-MPH 7- by 10-foot tunnel with and without ground-plane boundary-layer removal. Trim characteristics were determined for the model with and without landing gear. An analytical study showing the effect of airplane size on landing trajectories is also included.

No significant differences in the aerodynamic characteristics were indicated with ground-plane boundary layer present or removed. The increases in lift-curve slope and longitudinal stability and the reduction in induced drag usually encountered by an airplane entering ground effect were noted. A landing-flare motion analysis using the experimentally determined data has indicated the descent rate at touchdown for a large low-aspect-ratio wing airplane of the supersonic transport size would be less than for a small airplane during a constant pitch attitude approach due to the longer time spent in ground effect. The descent rates encountered at touchdown were excessive for normal operational landings.

INTRODUCTION

Recent developments in moving-belt ground simulation techniques have removed some test uncertainties which have existed for wind-tunnel investigations of models in the presence of a ground boundary. (See ref. 1.) In simulating the actual flight conditions of an airplane moving over the ground, the use of a moving-belt ground plane (to eliminate the boundary layer) has been shown to be desirable for configurations employing high-lift devices close to the ground plane. These results, which are not well defined at low-lift coefficients, imply that boundary-layer removal is unessential for models operating at relatively low-lift coefficients. In order to verify this implication and to determine any other unknowns associated with testing low-aspect-ratio configurations in ground proximity, a model was investigated in the moving-belt facility described in reference 1.

The configuration selected for study was one in which ground-effect data were available from an investigation on a full-scale airplane. The airplane used in the flight investigation was an airplane modified to incorporate an ogee-wing planform. Results of the flight tests, together with some wind-tunnel tests of the full-scale airplane and some preliminary results of this investigation, are reported in reference 2.

The present investigation utilized a 0.15-scale model of the full-scale airplane. Wind-tunnel studies were made in the Langley 300-MPH 7- by 10-foot tunnel at a Mach number of 0.079, which corresponds to a Reynolds number of about 2.15×10^6 based on the mean aerodynamic chord. The model was tested over the moving-belt ground-plane facility (ref. 1) at heights above the moving belt varying from 1.063 to 0.27 reference chords. The tests were made with and without the ground plane moving to determine the effect of boundary-layer removal. Trim characteristics were obtained for the configuration both with and without the landing gear. This paper presents the detailed results of the model investigation as well as some analytical results to show the effect of airplane size on the rate of descent near touchdown.

SYMBOLS

The force and moment data are referred to the stability-axis system and the pitching-moment coefficients are referenced to a point located in the wing chord plane $1.194\bar{c}$ aft of the nose of the model. The model reference dimensions which were used in reducing the wind-tunnel data are given in figure 1.

Measurements for this investigation were taken in the U.S. Customary System of Units. Equivalent values are indicated parenthetically in the International System of Units (SI). Details concerning use of the SI, together with physical constants and conversion factors, are given in reference 3.

C_D drag coefficient, $\frac{\text{Drag}}{qS}$

$C_{D,0}$ drag coefficient at $C_L = 0$

C_L lift coefficient, $\frac{\text{Lift}}{qS}$

$C_{L,0}$ lift coefficient at $\alpha = 0^o$

C_{L_α} lift-curve slope per degree at $C_L \approx 0.45$

C_m	pitching-moment coefficient, $\frac{\text{Pitching moment}}{qS\bar{c}}$
$C_{m,0}$	pitching-moment coefficient at $C_L = 0$
$\partial C_D / \partial C_L^2$	drag-due-to-lift parameter
$\partial C_m / \partial C_L$	slope of the pitching-moment curve at $C_L \approx 0.45$
$\partial C_D / \partial \delta_e$ $\partial C_L / \partial \delta_e$ $\partial C_m / \partial \delta_e$	elevator deflection parameters, per degree
$\bar{c}$	wing mean aerodynamic chord
d	horizontal distance
g	acceleration due to gravity
h	height of model above the ground plane, measured from model moment reference to ground plane
dh/dt	rate of climb or descent
h_{gear}	height of airplane landing gear above the ground
I_y	moment of inertia about Y-axis
n	normal load factor
q	free-stream dynamic pressure
S	wing reference area

T	airplane thrust
t	time, sec
V	airplane velocity component tangent to flight path
dV/dt	rate of change of airplane velocity with time
V_B	speed of ground belt
V_∞	tunnel free-stream velocity
W	airplane weight
α	angle of attack, degrees
γ	flight-path angle, degrees
$d\gamma/dt$	rate of change of flight-path angle, radians/second
δ_e	elevator angle, degrees
θ	pitch attitude, degrees
$d^2\theta/dt^2$	angular acceleration in pitch, radians/second^2
ρ	density of air

Subscript:

o	initial condition

MODEL AND TEST APPARATUS

The basic model used in the investigation was a 0.15-scale version of the Douglas F5D-1 airplane with the wing leading edge and duct intakes extended forward to provide

an ogee planform as shown in figure 1. The resulting planform, with the exception of the outboard elevon trailing edges, was geometrically similar to that of the full-scale airplane discussed in reference 2. The elevon trailing edges of the model extended to the tip whereas the airplane elevons were rounded off. Additional modifications were made to the top of the fuselage; the existing fairing between the canopy and the vertical tail was replaced by one large enough to accommodate the balance and sting as shown in figure 1.

The investigation was made in the 17-foot test section of the Langley 300-MPH 7- by 10-foot tunnel, utilizing the moving-belt ground plane described in reference 1. The model, which was sting supported, is shown in figures 1 and 2. Figure 3 shows a photograph of the moving belt and model-support installation. Forces and moments were measured from an internally mounted six-component strain-gage balance.

TESTS

The tests were made at a free-stream dynamic pressure of 9.02 pounds/foot^2 (1.88 newtons/meter^2) which corresponds to a Mach number of about 0.079 and a Reynolds number of about 2.15×10^6 based on the model reference chord.

The model was tested through an angle-of-attack range from -4° to approximately 20° for values of $h/\bar{c}$ from 1.063 to 0.40; for smaller values of $h/\bar{c}$ (0.34 and 0.27) the angle-of-attack range was reduced to avoid model contact with the moving-belt ground plane. For these tests the distance from the ground plane to the model center of rotation (approximately the moment reference point, see fig. 1) was held constant at a predetermined value as the model was rotated through the angle-of-attack range. The possibility that the model characteristics might be affected by the ground-plane boundary layer was eliminated by operating the belt at free-stream velocity $(V_B = V_\infty)$ for all model heights corresponding to $h/\bar{c} < 0.75$; however, some additional tests were made with the belt inoperative $(V_B = 0)$ to determine any influence that the boundary layer might have on the characteristics.

During the investigation some unsteadiness exhibited by the model over most of the angle-of-attack range was reflected in the quality of the data. The unsteadiness might be described as a low-frequency, high-amplitude oscillation, which damped out at times but was generally present while data were being recorded. An attempt to reduce the scatter by averaging several data points for a given angle of attack was partly successful. As a result the plotted data represent the average value of five data points.

The drag coefficients have been corrected for momentum losses resulting from airflow through the model-engine ducts. Corrections have also been made to the angle of attack to account for the combined deflection of balance- and model-support system

due to aerodynamic loads. Variations in model height due to aerodynamic load were eliminated by repeated model-support height adjustments.

DISCUSSION

Experimental Results

Effect of moving ground plane.- The effect of ground-plane boundary layer on the aerodynamics of the model is shown in figure 4. The results indicate no significant differences in the characteristics obtained with the ground-plane belt stationary $(V_B = 0)$ or with the ground-plane belt operating at a speed equivalent to free-stream velocity $(V_B = V_\infty)$. These findings are in accordance with results of reference 1 which indicate the moving-ground technique is unnecessary for wings operating at relatively low lift coefficients. These results, however, may not be compatible with those obtained from other facilities, where differences in the nature of the boundary-layer profiles above the ground plane might exist.

Effect of model height.- The effect of model height above the moving belt on the aerodynamic characteristics of the configuration having landing gear off and elevons undeflected is also shown in figure 4. The increases in lift-curve slope and longitudinal stability and the reduction in induced drag usually encountered when an airplane enters a region of ground effect are noted as the model height is reduced from $h/\bar{c} = 1.063$ to $h/\bar{c} = 0.27$. From the elevon characteristics presented in figure 5 it will also be noted that there is a positive shift in the zero-lift pitching-moment coefficient as the model height is reduced. In a landing maneuver this characteristic will tend to compensate for the increased elevator deflection required for trim resulting from the increased longitudinal stability.

Effect of landing gear.- The effect of addition of the landing gear on the aerodynamic characteristics of the model is shown in figure 6 and elevon characteristics (landing gear on) are presented in figure 7. No significant differences in the characteristics of the two configurations appear other than the increment in drag coefficient (approximately 0.01) due to the addition of the landing gear.

Landing-Flare Motion Analysis

A three-degree-of-freedom-motion study was made to determine the landing-flare trajectory for a configuration having characteristics representative of the full-scale fighter-type airplane and for a configuration with the same aerodynamic characteristics but having the size of a supersonic transport. For the purpose of this analysis the aerodynamic parameters were plotted as a function of $h/\bar{c}$ as shown in figure 8 and were used as inputs to a computer programed with the longitudinal equations of motion. The

parameters C_{L_α} and $C_{L,0}$ are, respectively, the slope of the tangent to the lift curve at $C_L \approx 0.45$ and its intercept at $\alpha = 0^o$. The pitching-moment parameter $\partial C_m/\partial C_L$ and the induced drag parameters $\partial C_D/\partial C_L^2$ represent the slopes of their respective curves over a wide lift-coefficient range ($C_L = 0$ to $C_L \approx 0.55$). The pitching-moment coefficient was taken as the intercept of $\partial C_m/\partial C_L$ at $C_L = 0$. The drag coefficient was obtained from unpublished data on the full-scale fighter-type airplane. The elevon parameters which show no significant effect of model height were measured at $C_L \approx 0.45$.

Physical characteristics and initial conditions for the configurations considered in this analysis are given in table I. The aircraft motions that occur in execution of the landing flare are shown in sketch A. For the initial conditions both airplanes were assumed to be in steady unaccelerated flight along a 3^o glide slope in the approach configuration (landing gear down). Landing trajectories were then obtained for each airplane in constant pitch attitude and fixed elevon approaches.

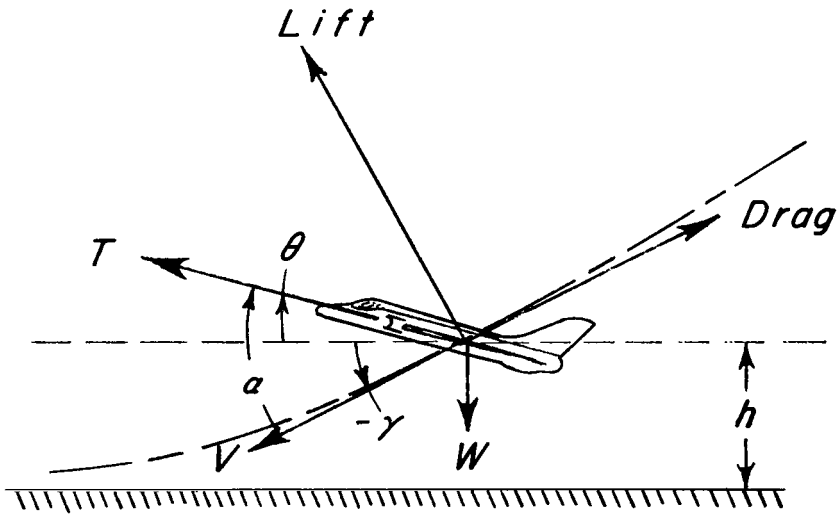

Sketch A.

The equations of motion that follow were used in this analysis. The change in flight-path angle per unit time is given by

$$\frac{d\gamma}{dt} = \frac{g}{V}\left[C_L \frac{\rho V^2}{2W/S} - \cos\gamma + \frac{T}{W}\sin\alpha\right] \tag{1}$$

where

$$C_L = C_{L,0} + C_{L_\alpha}\alpha + \frac{\partial C_L}{\partial \delta_e}\delta_e$$

The landing approach acceleration is expressed as

$$\frac{dV}{dt} = g\left[\frac{T}{W}\cos\alpha - \frac{C_D \rho V^2}{2W/S} - \sin\gamma\right] \tag{2}$$

where

$$C_D = C_{D,0} + \frac{\partial C_D}{\partial C_L{}^2} C_L{}^2 + \frac{\partial C_D}{\partial \delta_e}\delta_e$$

Pitching acceleration is given as

$$\frac{d^2\theta}{dt^2} = \frac{C_m \rho V^2 S\bar{c}}{2I_y} \tag{3}$$

where

$$C_m = C_{m,0} + \frac{\partial C_m}{\partial C_L} C_L + \frac{\partial C_m}{\partial \delta_e}\delta_e$$

As is indicated in sketch A,

$$\theta = \alpha + \gamma \tag{4}$$

$$\frac{dh}{dt} = V \sin\gamma \tag{5}$$

The results of the analytical study of the landing trajectories are presented in figures 9 and 10. These results indicate that for a constant-pitch-attitude flare from an initial descent rate of 12 feet/second (3.66 meters/second), touchdown descent rates of 9.4 feet/second (2.87 meters/second) were obtained for the small airplane and 6.8 feet/second (2.07 meters/second) for the supersonic transport airplane. The smaller rate of descent for the larger airplane results from the longer time spent in the region of ground effects even though the maximum normal acceleration in the flare was considerably lower for the airplane having dimensions of the supersonic transport. This point is further illustrated in figure 10, wherein the effect of ground proximity is noted at $h/\bar{c}$ slightly less than 1.0 which corresponds to a landing-gear height above the ground of about 17 feet (5.18 meters) for the fighter-type airplane and about 60 feet (18.29 meters) for the supersonic transport. Although the rate of descent of the large airplane has been reduced in the constant-attitude flare the rate of descent at touchdown 6.8 feet/second (2.07 meters/second) is excessive for normal operational landings and is considerably higher than the rate of 2 feet/second (0.61 meter/second) anticipated in reference 4 for a low-aspect-ratio supersonic transport airplane.

Examination of the fixed-elevator approaches for the two configurations when ground effect is encountered indicates buildups in normal load factor similar to those noted for the constant-pitch-attitude approaches which initially reduce descent rates. These initial trends are the result of the favorable effect of the increasing lift-curve slope, which begins at $h/\overline{c} \approx 1.0$ as noted in figure 8(a). However, as the airplane descent continues, the adverse effect of increasing longitudinal stability is encountered (fig. 8(c)). The increasing negative value of $\partial C_m/\partial C_L$ reduces pitch attitude and results in the pronounced reversal in normal load factor and an increase in touchdown descent rates noted particularly for the supersonic transport configuration.

CONCLUSIONS

A wind-tunnel investigation of a low-aspect-ratio ogee-wing model in ground proximity with and without ground-plane boundary-layer removal has indicated the following conclusions:

No significant differences in the longitudinal aerodynamic characteristics of the model were indicated with the ground-plane boundary layer present or with it removed. The increases in lift-curve slope and longitudinal stability and the reduction in induced drag usually encountered by an airplane entering ground effect were noted. A landing-flare motion analysis using the experimentally determined characteristics has indicated the descent rate at touchdown for a large airplane with a low-aspect-ratio wing (of the dimensions of a supersonic transport) would be less than for a small airplane during a constant-pitch-attitude approach because of the longer time spent in ground influences. The descent rates encountered at touchdown, however, would be excessive for normal operational landing.

Langley Research Center,
National Aeronautics and Space Administration,
Langley Station, Hampton, Va., June 14, 1967,
720-01-00-03-23.

REFERENCES

1. Turner, Thomas R.: A Moving-Belt Ground Plane for Wind-Tunnel Ground Simulation and Results for Two Jet-Flap Configurations. NASA TN D-4228, 1967.

2. Rolls, L. Stewart; and Koenig, David G.: Flight-Measured Ground Effect On a Low-Aspect-Ratio Ogee Wing Including a Comparison With Wind-Tunnel Results. NASA TN D-3431, 1966.

3. Mechtly, E. A.: The International System of Units – Physical Constants and Conversion Factors. NASA SP-7012, 1964.

4. Magruder, W. M.; and McDonald, J. F.: Operating Techniques and Maintenance Practices for the Lockheed SST. [Preprint] 660295, Soc. Automotive Engrs., Apr. 1966.

TABLE I

CONSTANTS AND INITIAL CONDITIONS

Parameter	Full-scale fighter	Supersonic transport
S	661.00 ft^2 (61.407 m^2)	8 000.00 ft^2 (743.20 m^2)
$\bar{c}$	22.59 ft (6.885 m)	78.59 ft (23.954 m)
W	23 000 lb (10 433 kg)	278 400 lb (126 282 kg)
Aspect ratio	1.70	1.70
T/W	0.1920	0.1920
I_y	83.5×10^3 slug-ft^2 (11.32×10^4 kg-m^2)	17.4×10^6 slug-ft^2 (23.6×10^6 kg-m^2)
V_o	135.75 knots	135.75 knots
h_o	75.00 ft (22.86 m)	100.00 ft (30.48 m)
$\left(\frac{dh}{dt}\right)_o$	-12.00 ft/sec (3.658 m/sec)	-12.00 ft/sec (3.658 m/sec)
γ_o	-3.00^o	-3.00^o
θ_o	10.08^o	10.08^o
$\delta_{e,o}$	-3.65^o	-3.65^o

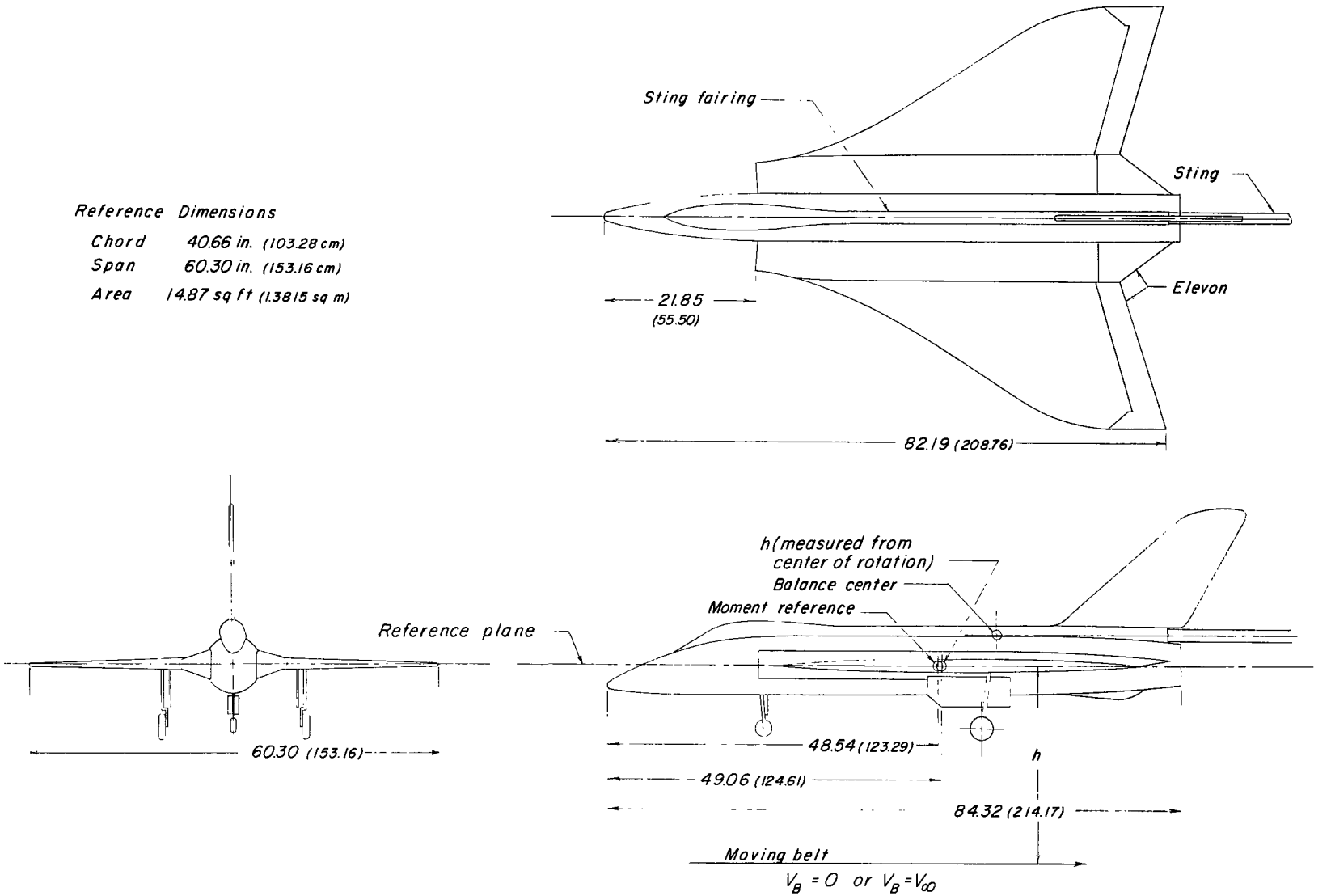

Figure 1.- Drawing of 0.15-scale model of a fighter-type airplane with NASA ogee-wing planforms. All linear dimensions are in inches (centimeters).

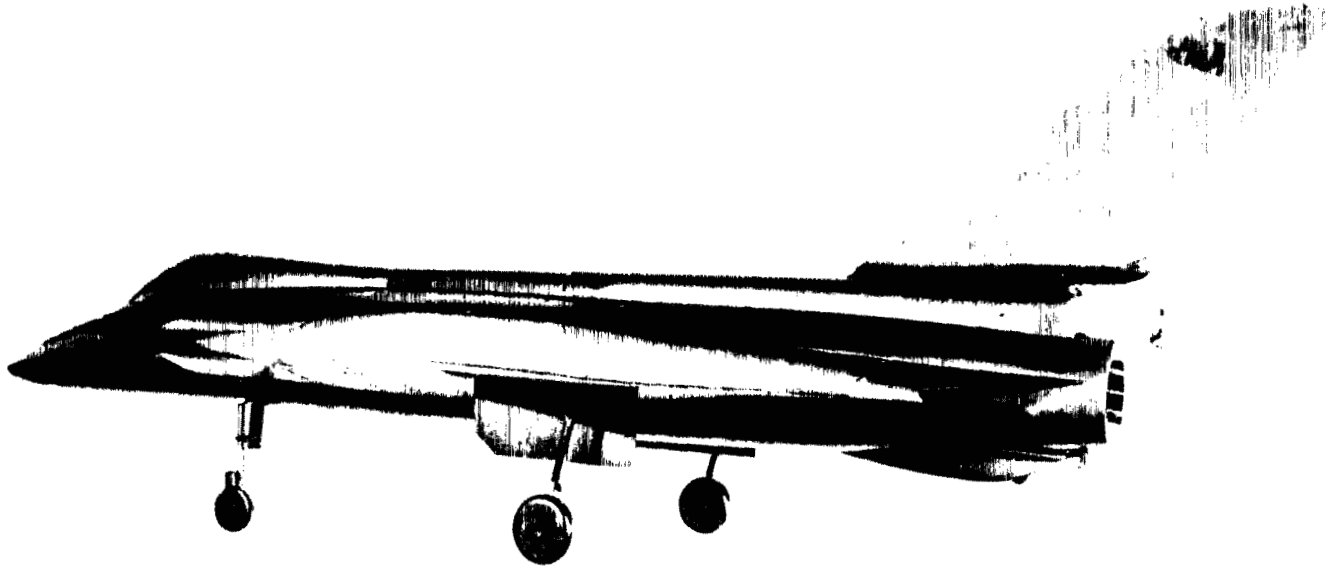

Figure 2.- Photograph of model.

L-65-5827

Figure 3.- Photograph of moving-belt ground plane in 17-foot test section.

L-66-1680

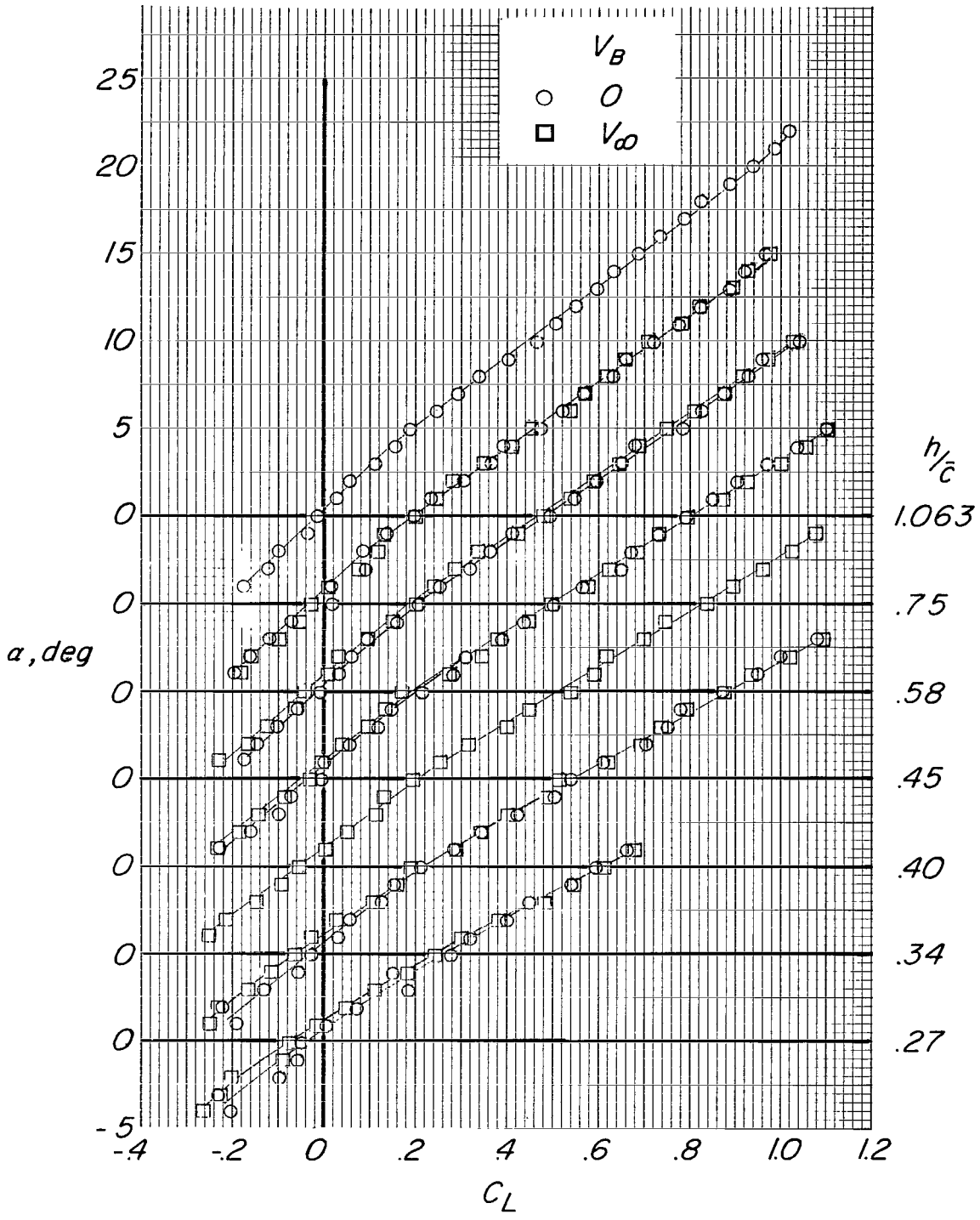

(a) α against C_L.

Figure 4.- Effect of model height and moving-belt ground plane on aerodynamic characteristics of model. Landing gear off.

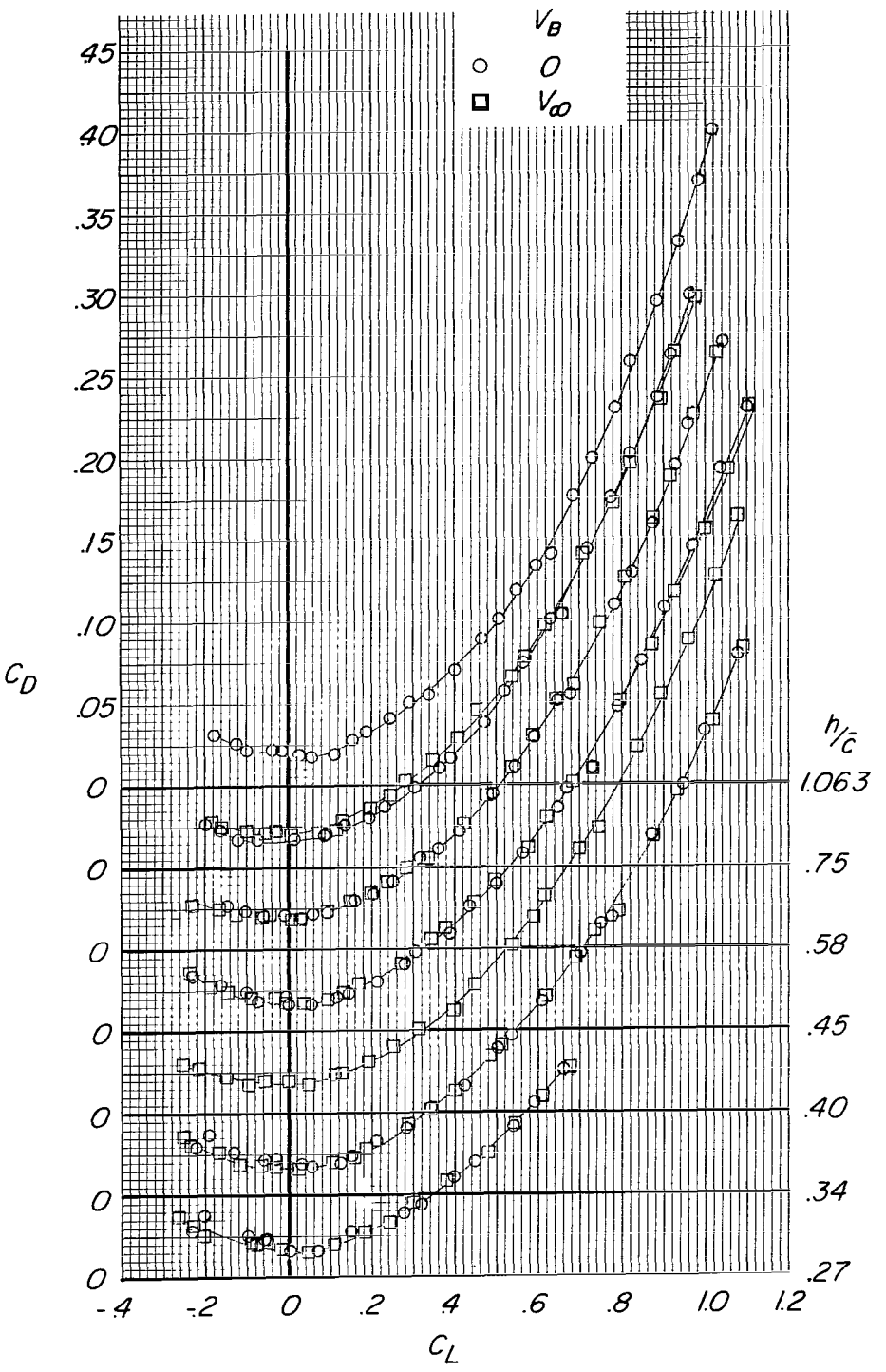

(b) C_D against C_L.

Figure 4.- Continued.

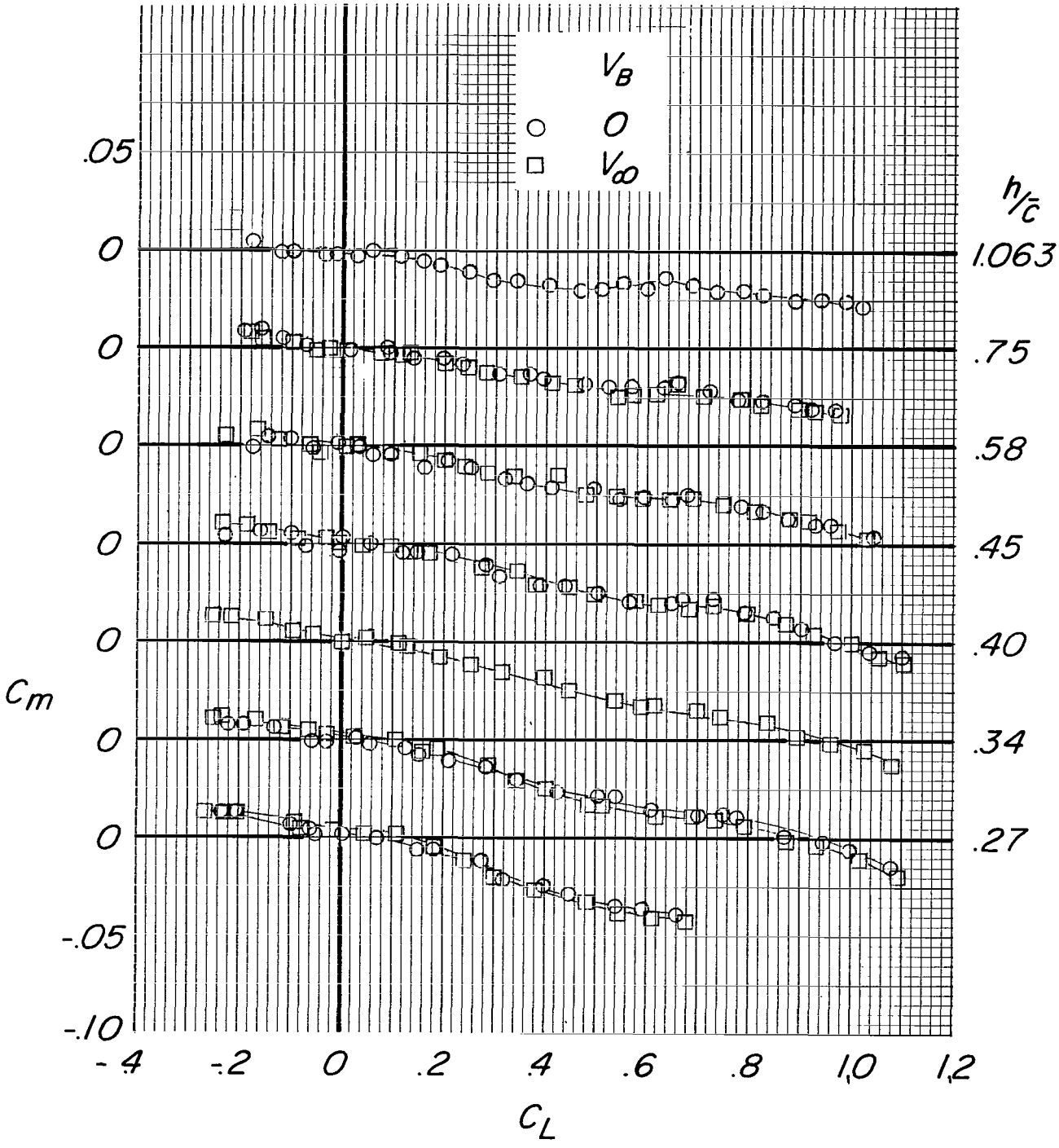

(c) C_m against C_L.

Figure 4.- Concluded.

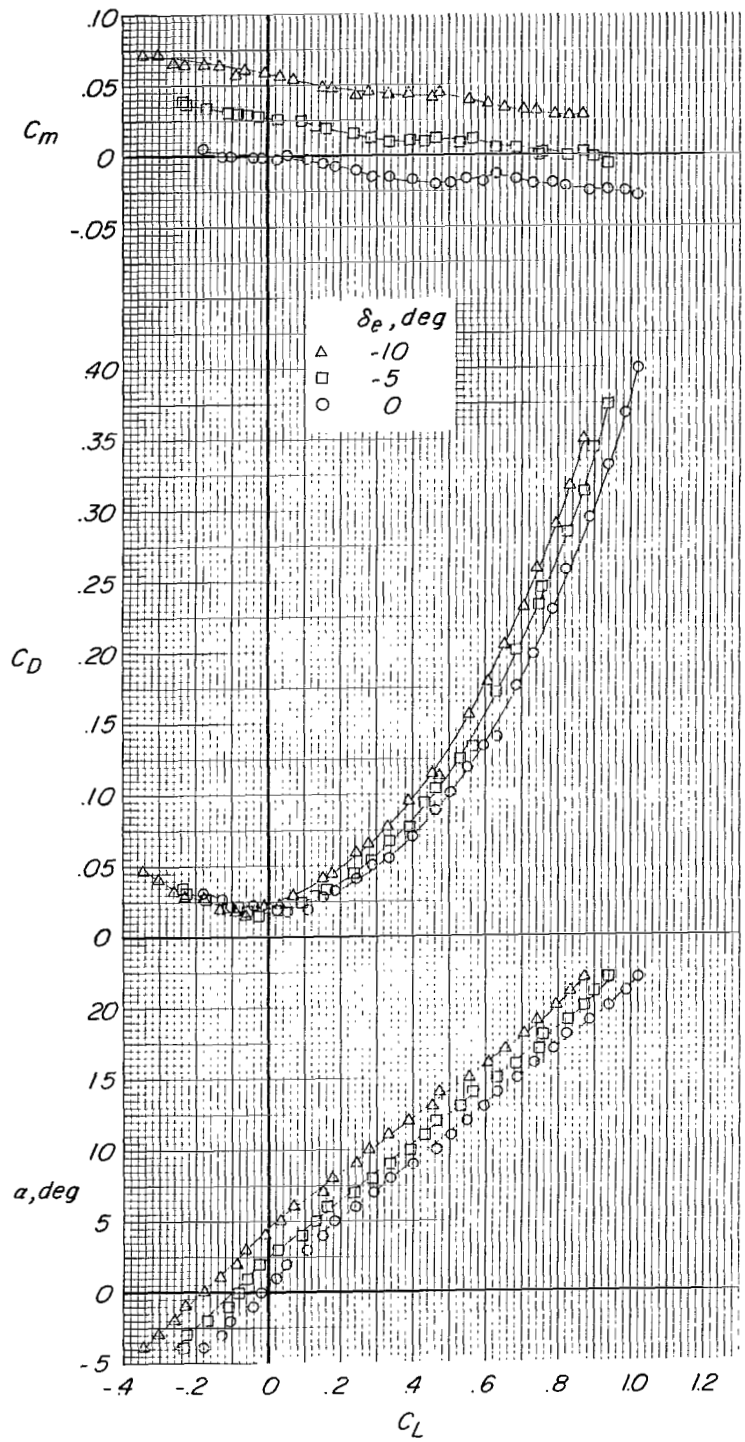

(a) $h/\bar{c} = 1.063$; $V_B = 0$.

Figure 5.- Effect of elevon deflection on aerodynamic characteristics in pitch. Landing gear off.

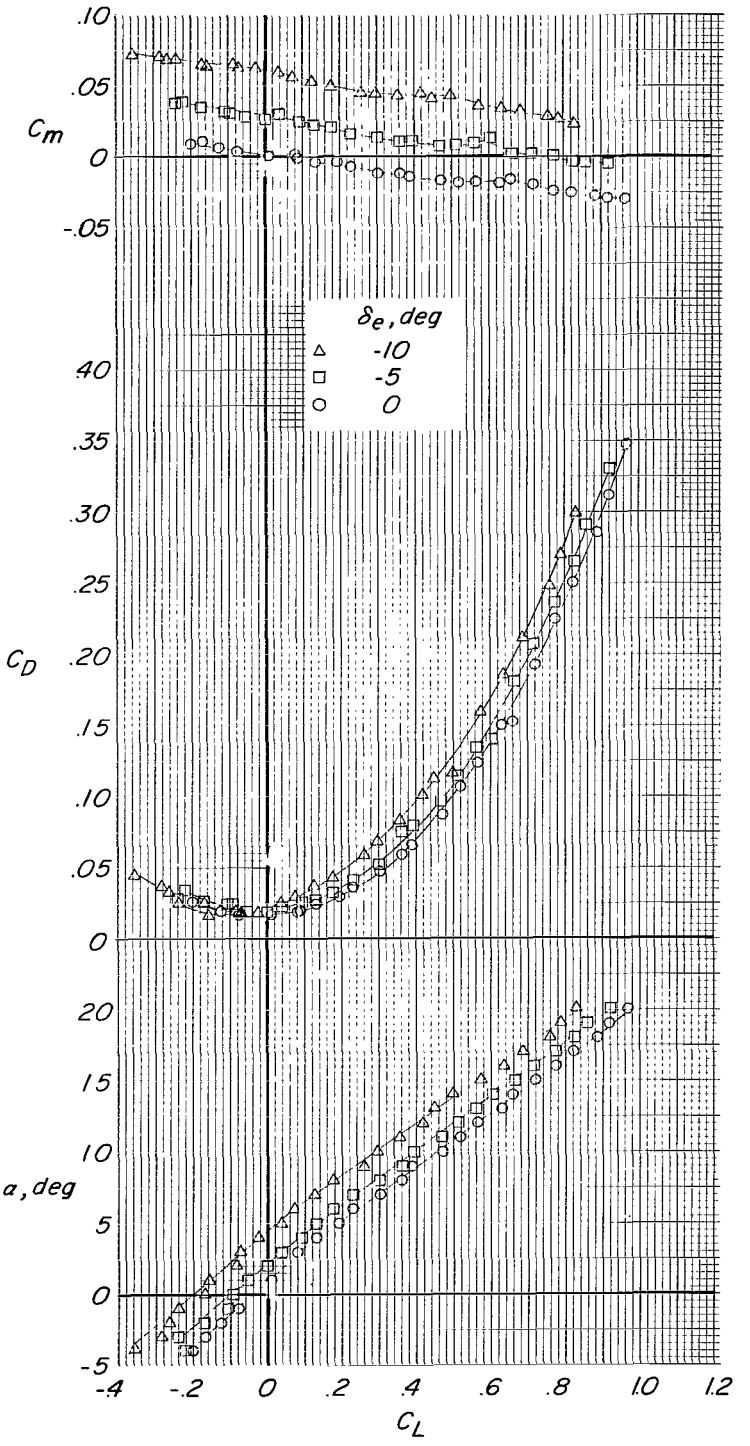

(b) $h/\bar{c} = 0.75$; $V_B = 0$.

Figure 5.- Continued.

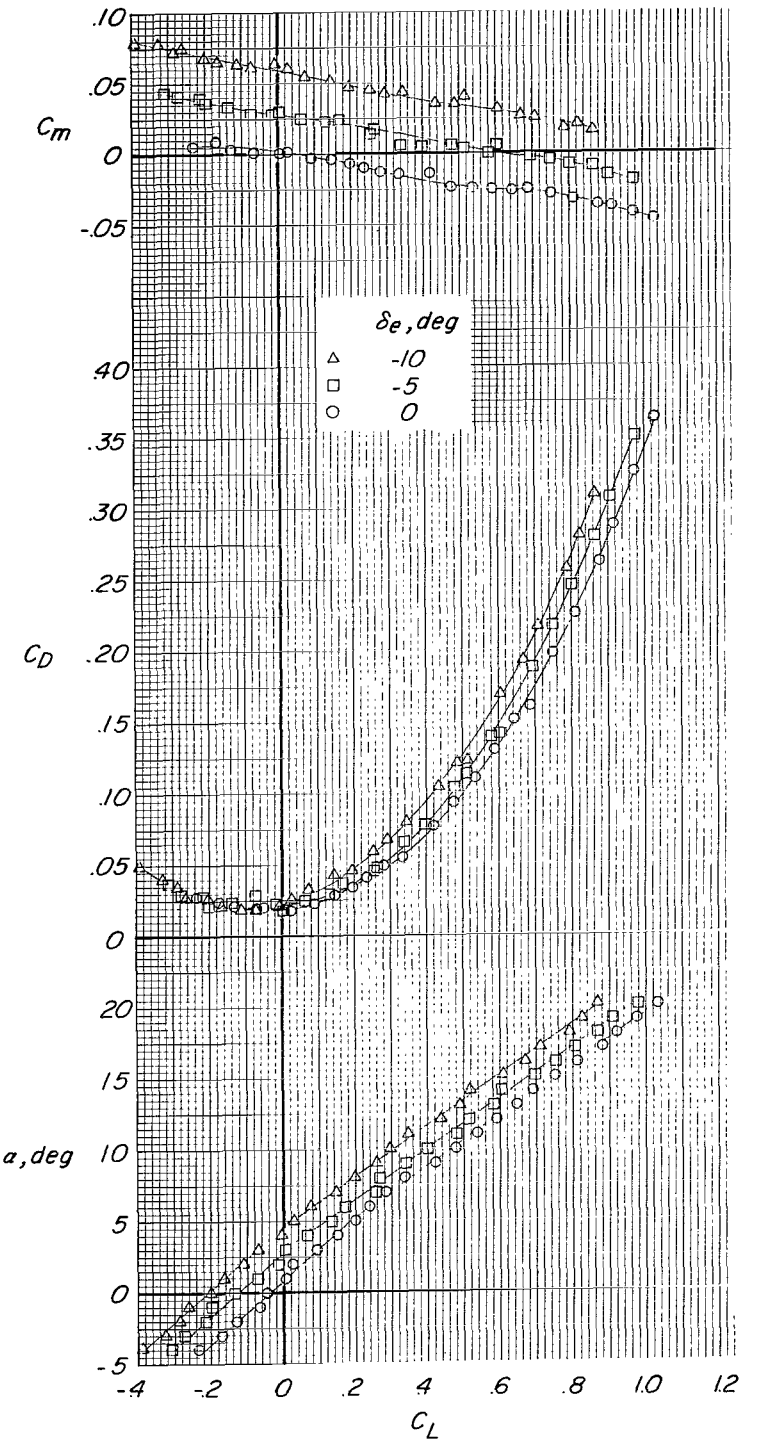

(c) $h/\bar{c} = 0.58$; $V_B = V_\infty$.

Figure 5.- Continued.

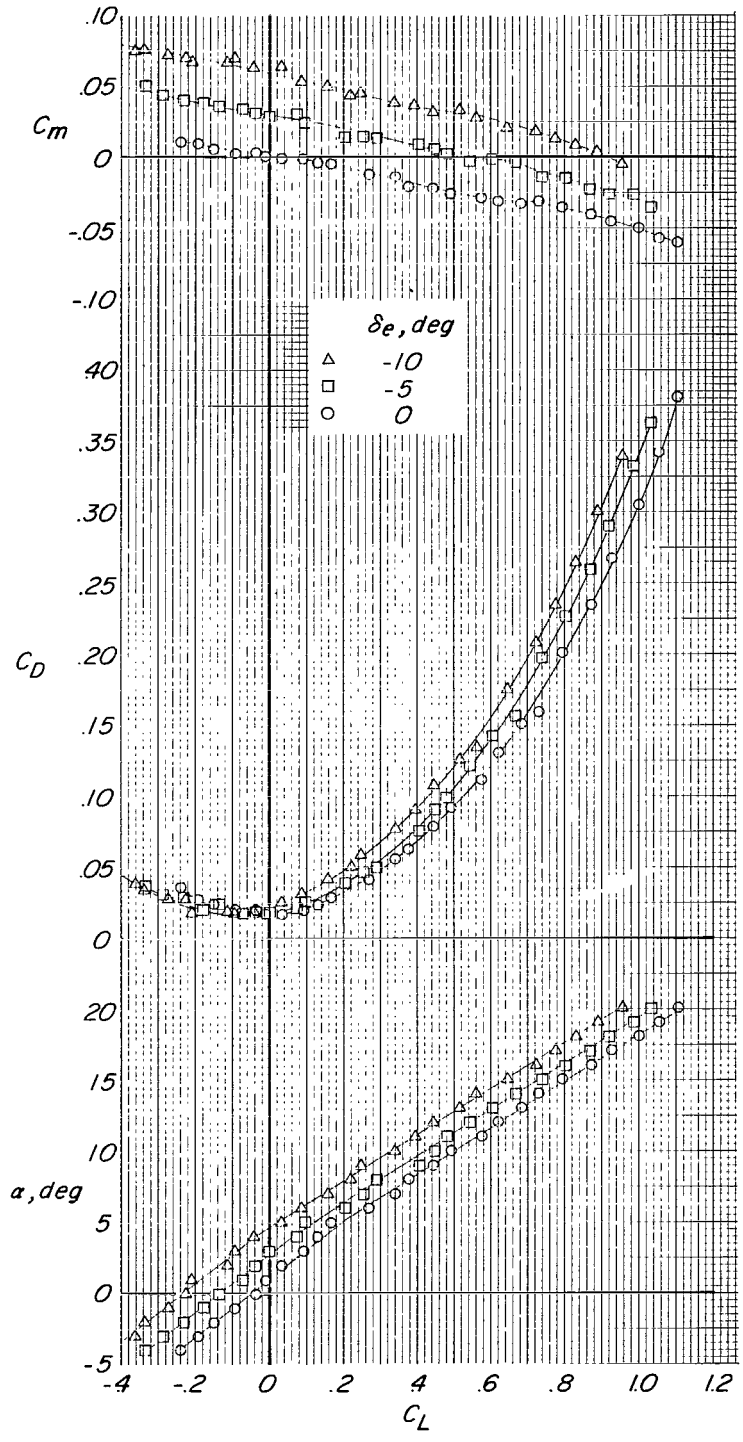

(d) $h/\bar{c} = 0.45$; $V_B = V_\infty$.

Figure 5.- Continued.

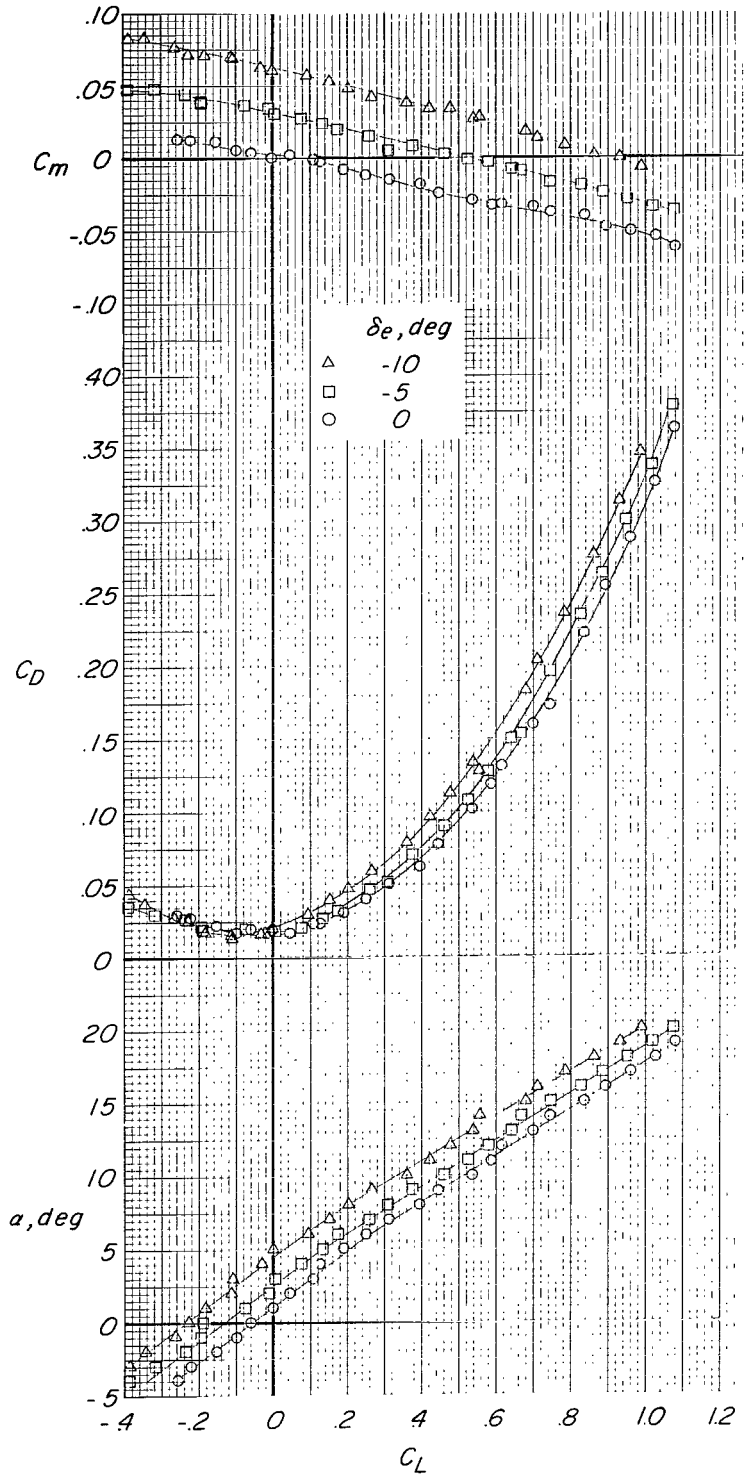

(e) $h/\bar{c} = 0.40$; $V_B = V_\infty$.

Figure 5.- Continued.

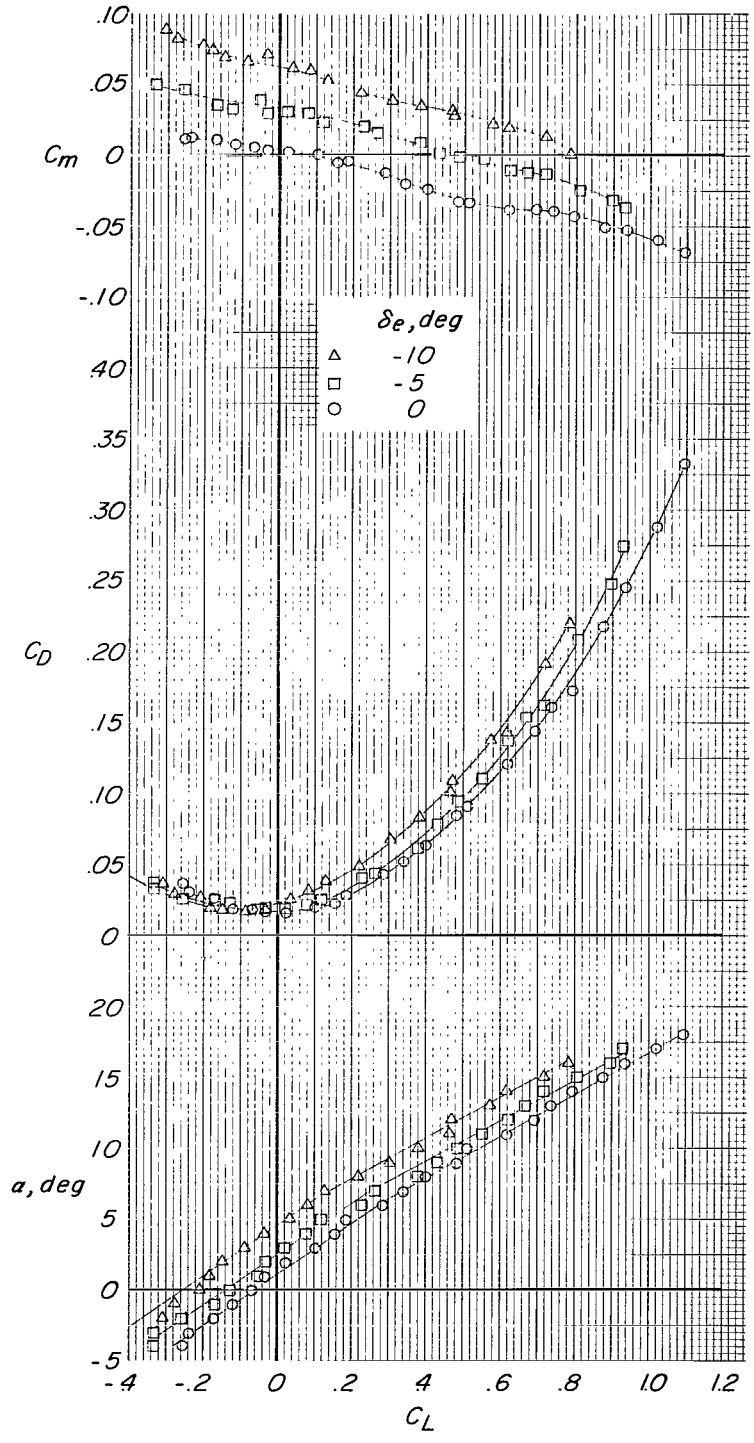

(f) $h/\bar{c} = 0.34$; $V_B = V_\infty$.

Figure 5.- Continued.

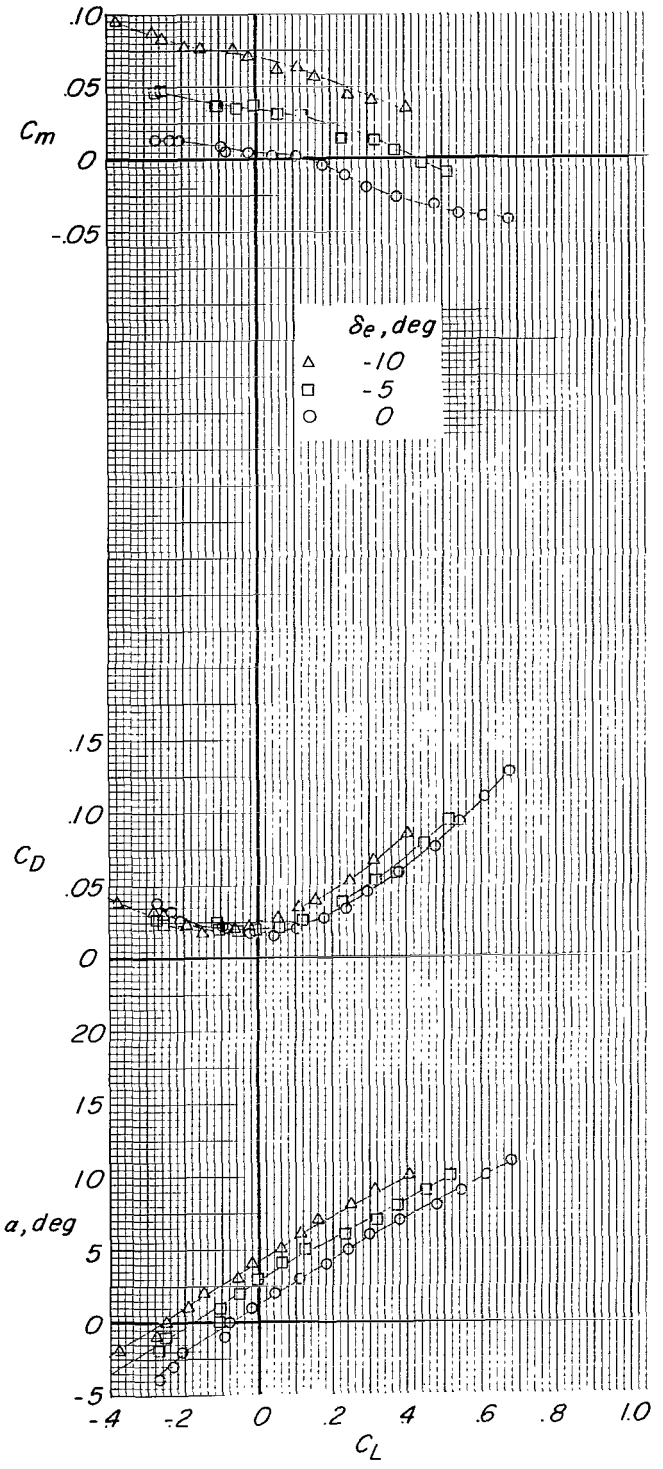

(g) $h/\bar{c} = 0.27$; $V_B = V_\infty$.

Figure 5.- Concluded.

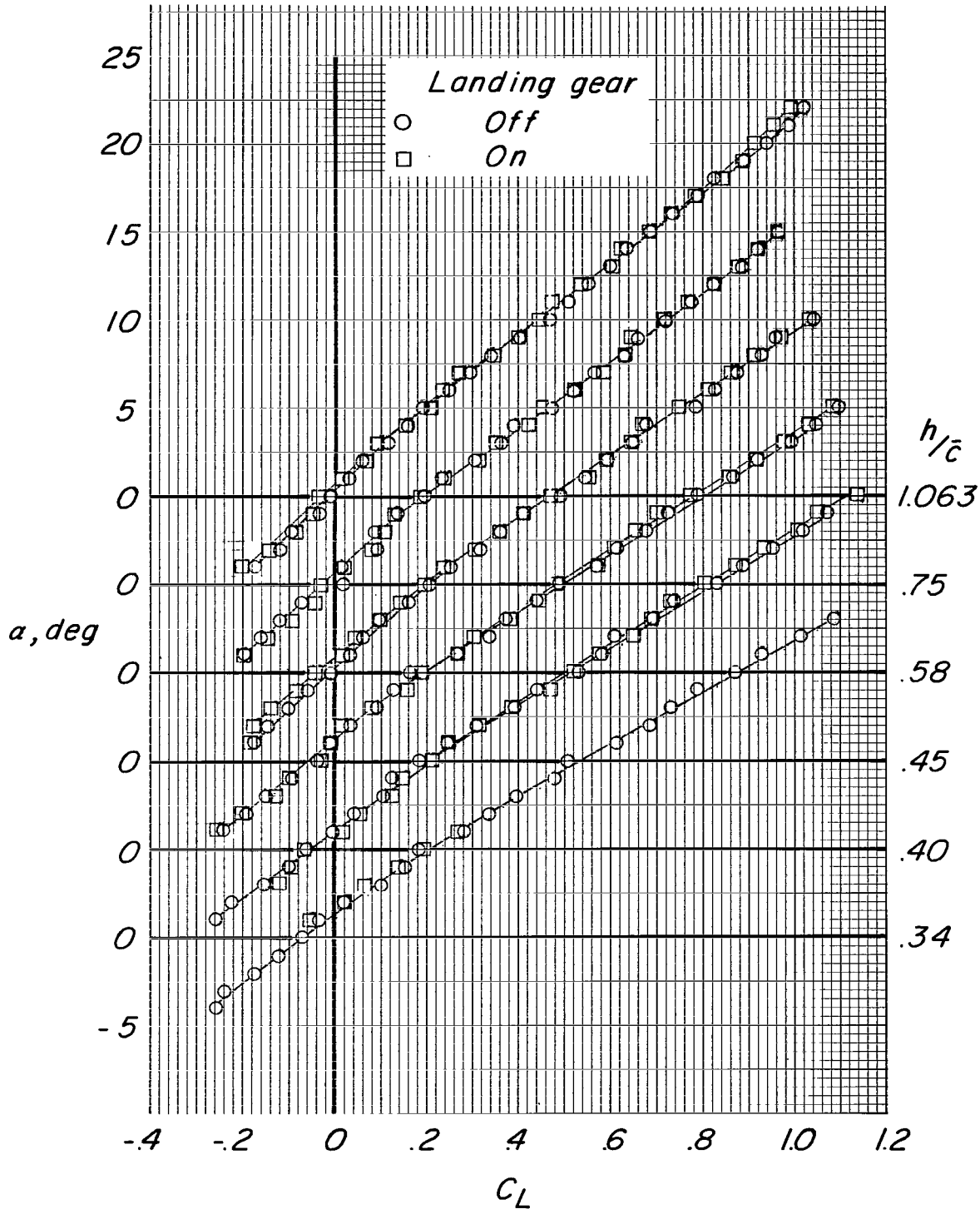

(a) α against C_L.

Figure 6.- Effect of model height and landing gear on the aerodynamic characteristics of model.

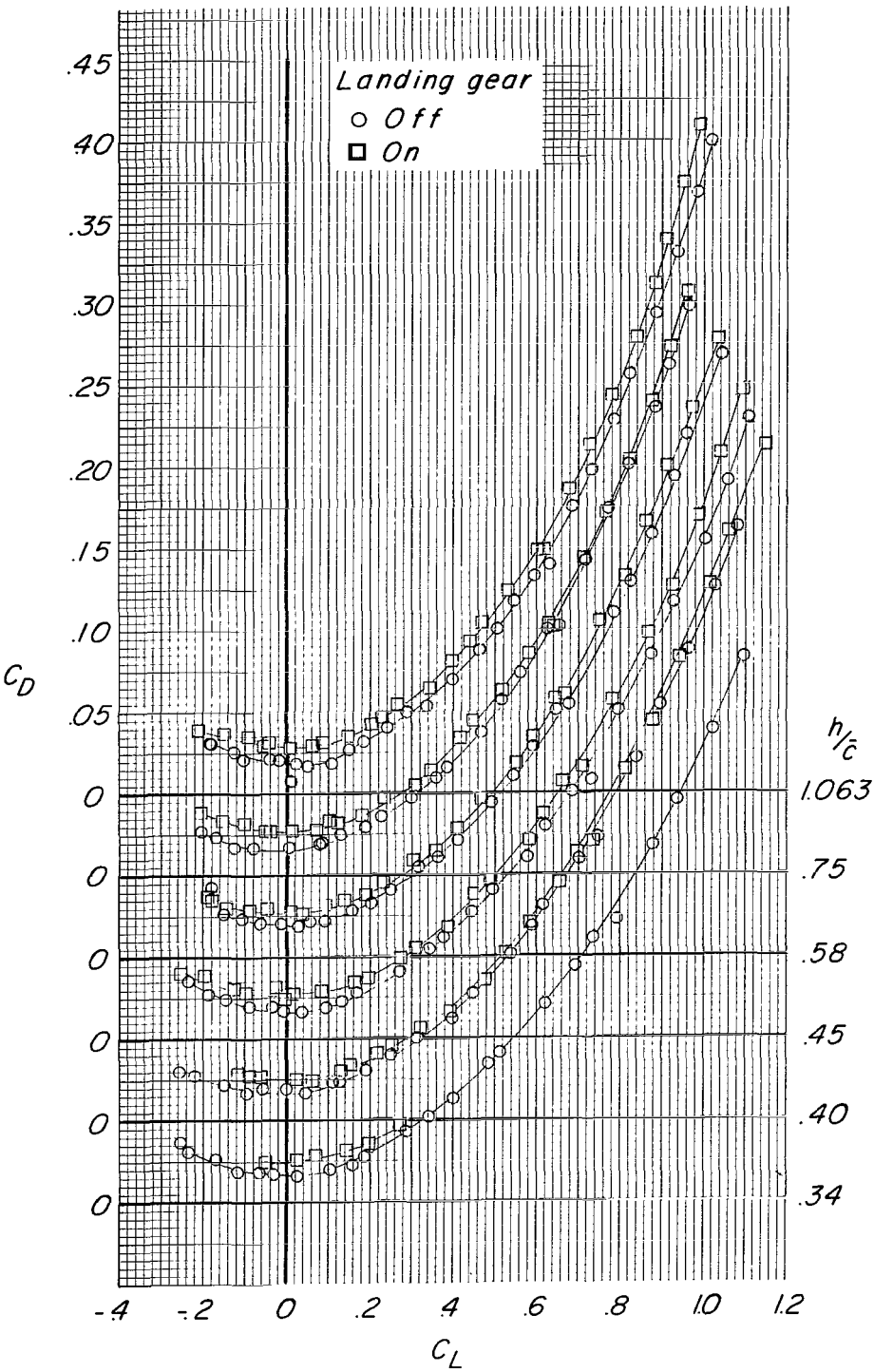

(b) C_D against C_L.

Figure 6.- Continued.

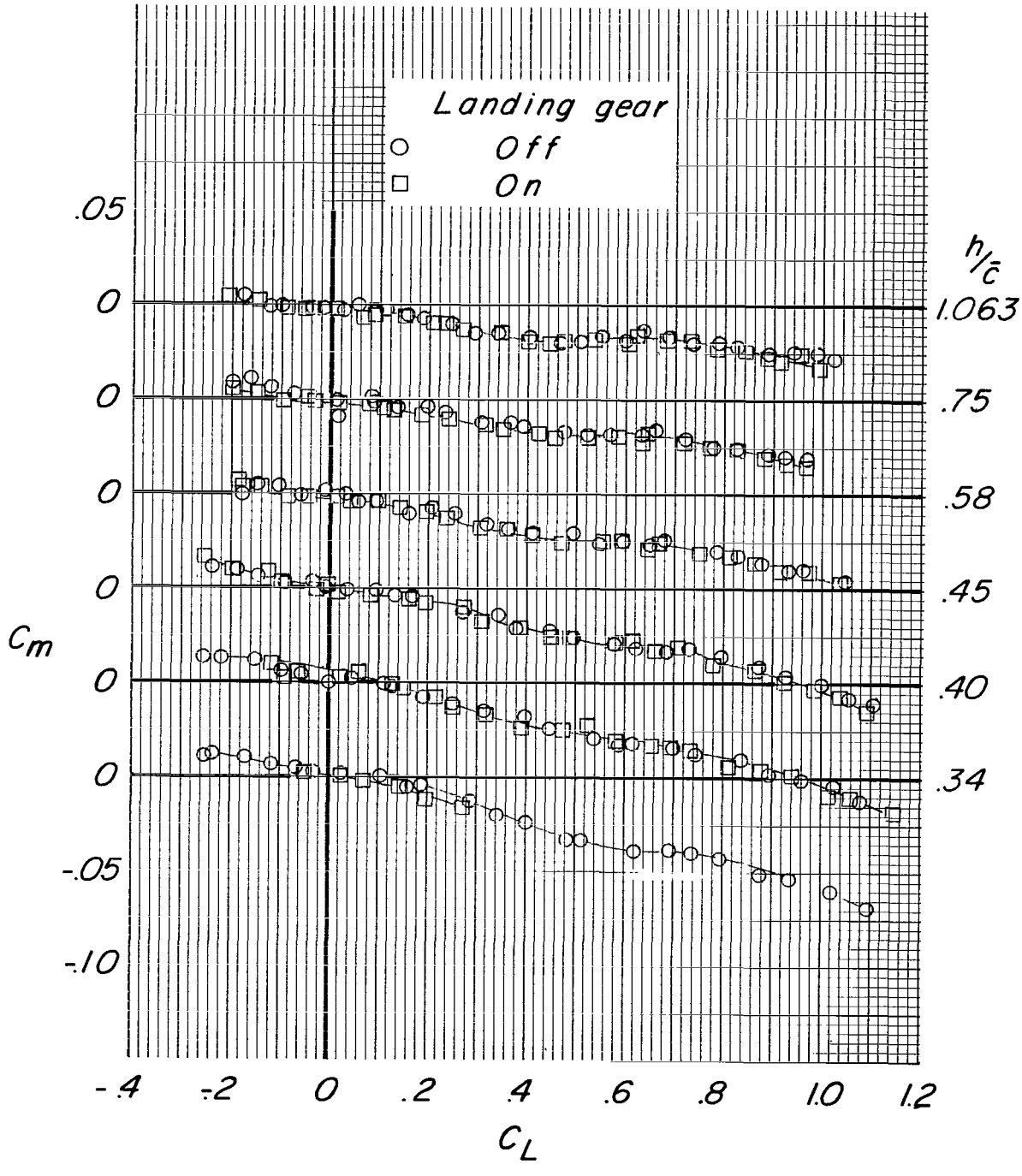

(c) C_m against C_L.

Figure 6.- Concluded.

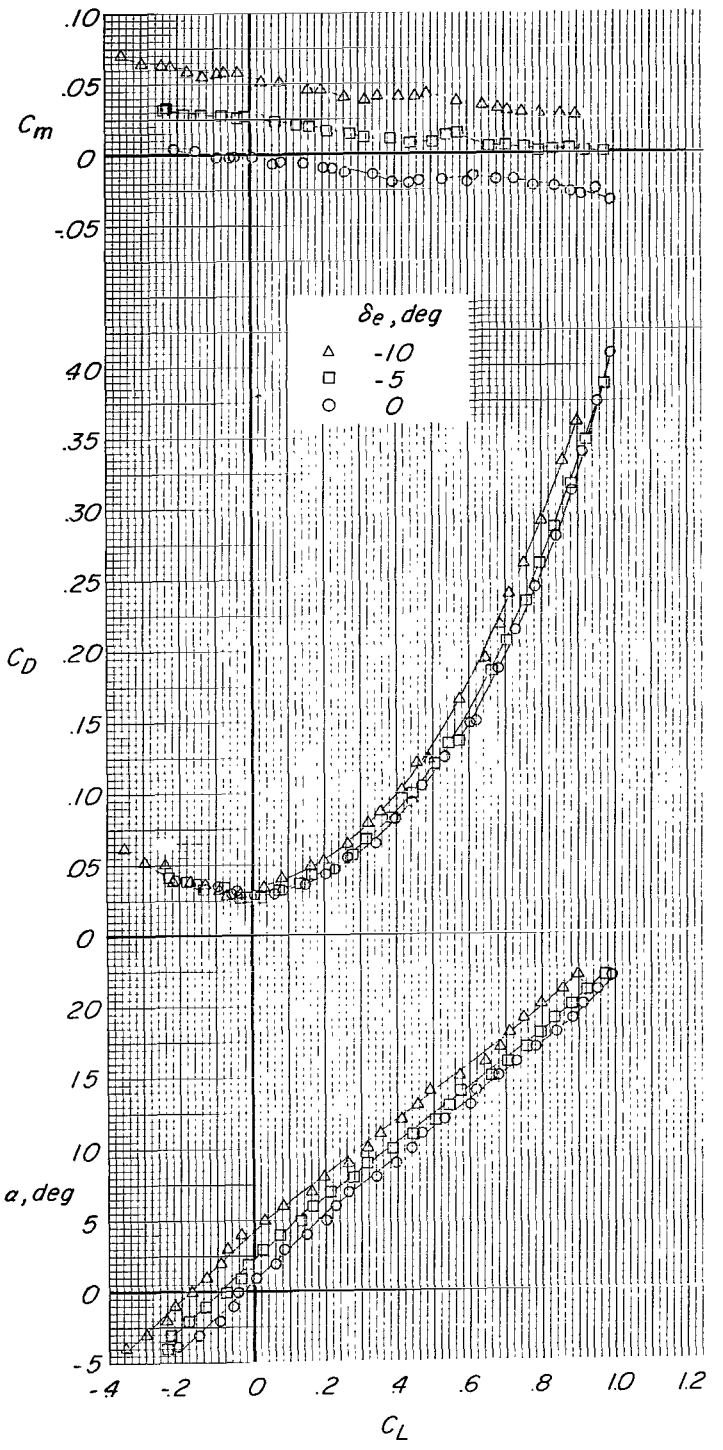

(a) $h/\bar{c} = 1.063$; $V_B = 0$.

Figure 7.- Effect of elevon deflection on the aerodynamic characteristics in pitch. Landing gear on.

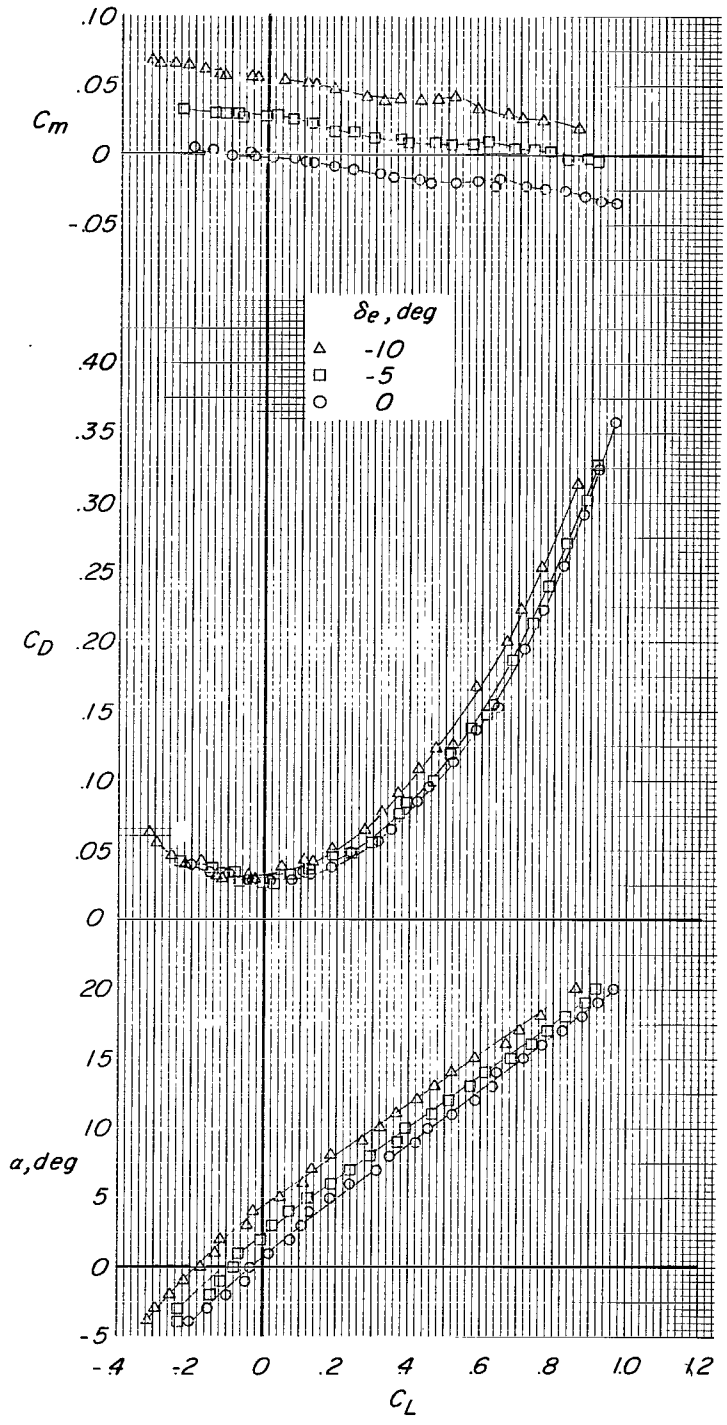

(b) $h/\bar{c} = 0.75$; $V_B = 0$.

Figure 7.- Continued.

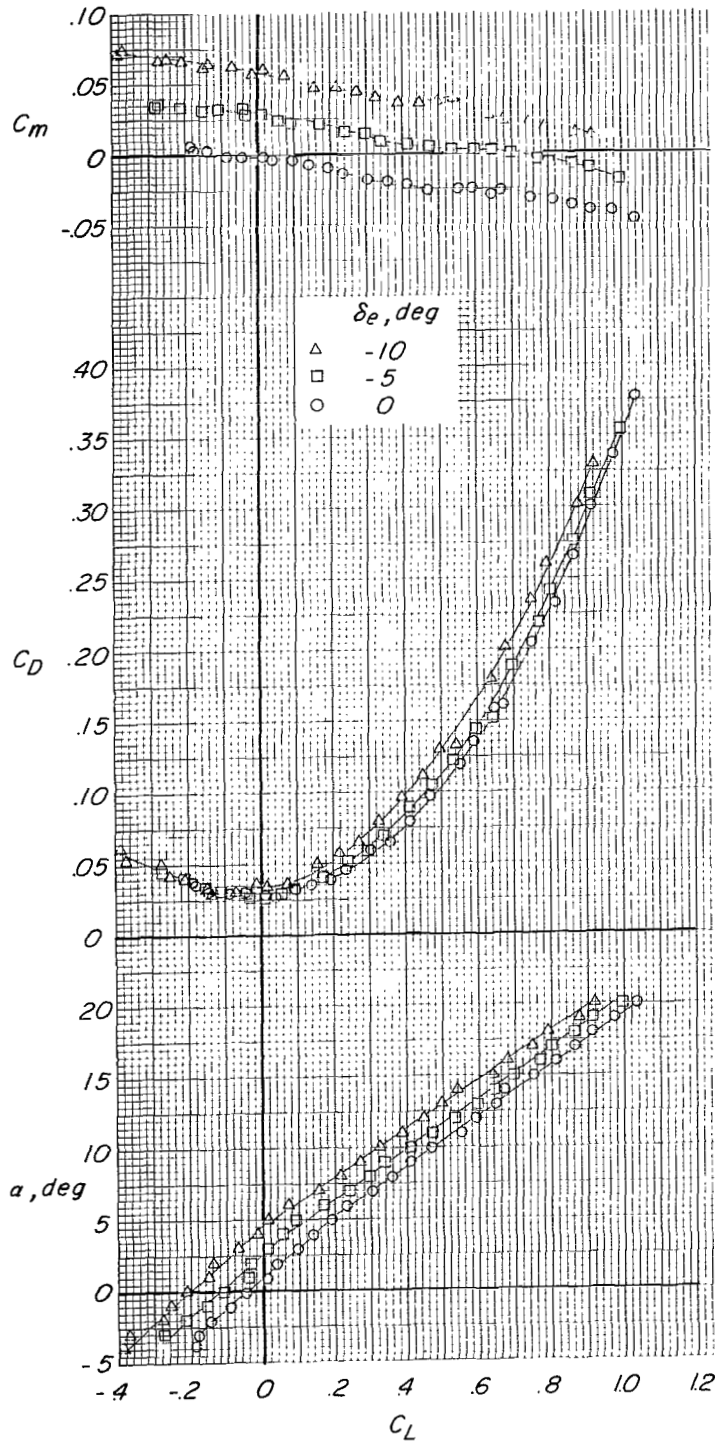

(c) $h/\bar{c} = 0.58$; $V_B = V_\infty$.

Figure 7.- Continued.

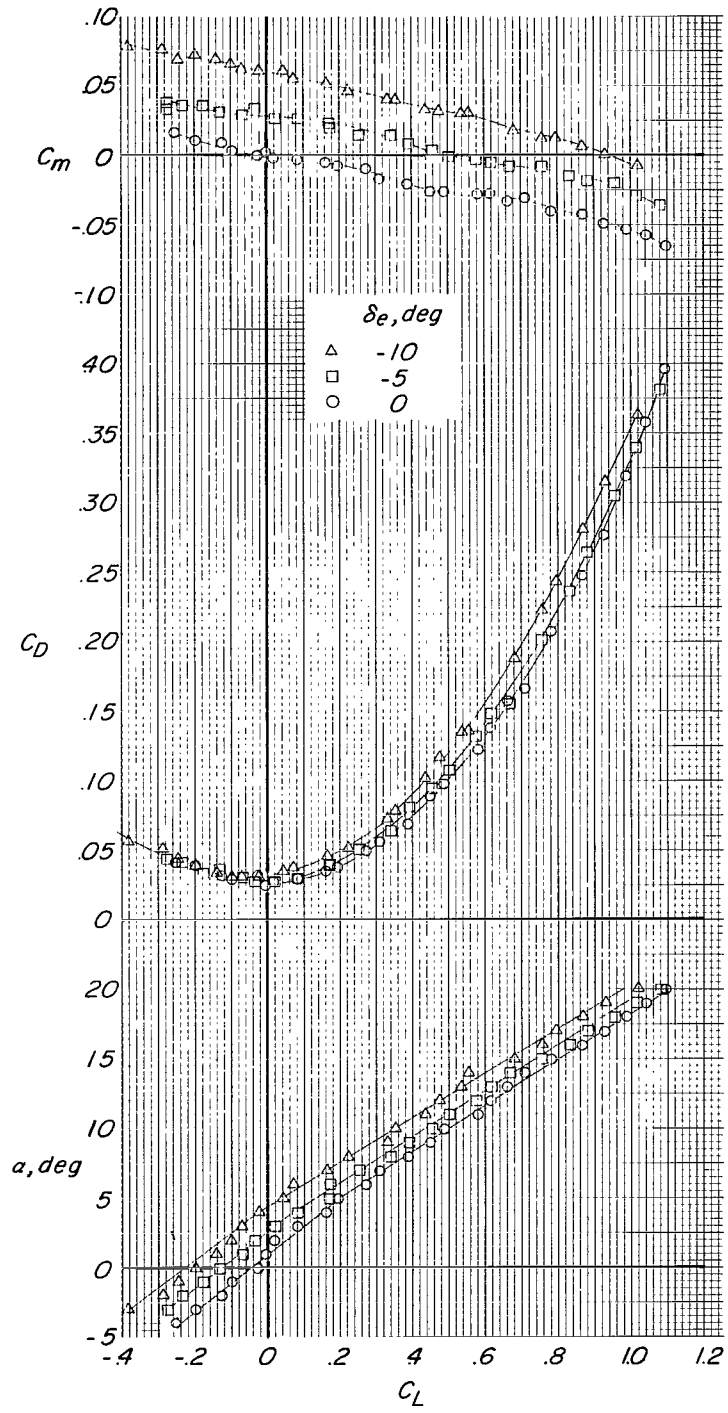

(d) $h/\bar{c} = 0.45$; $V_B = V_\infty$.

Figure 7.- Continued.

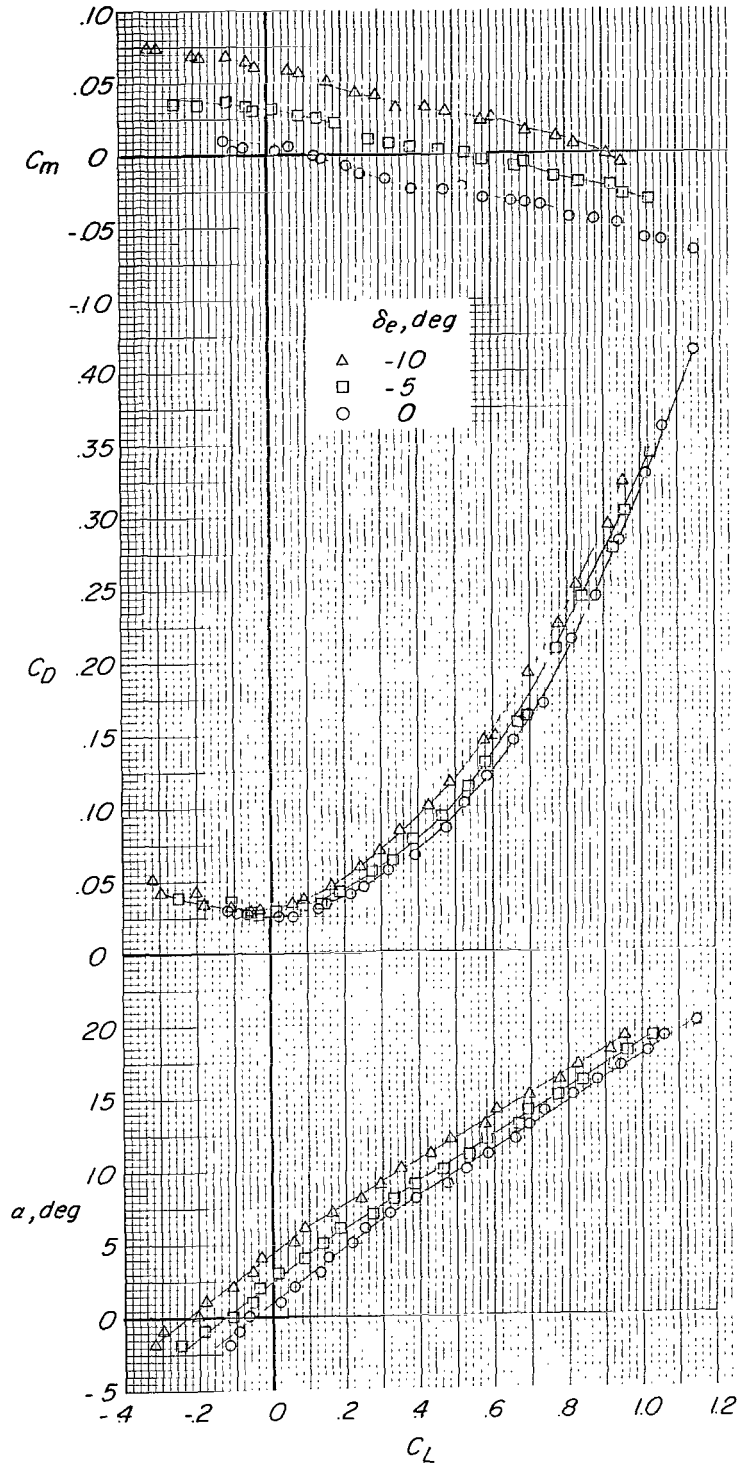

(e) $h/\bar{c} = 0.40$; $V_B = V_\infty$.

Figure 7.- Concluded.

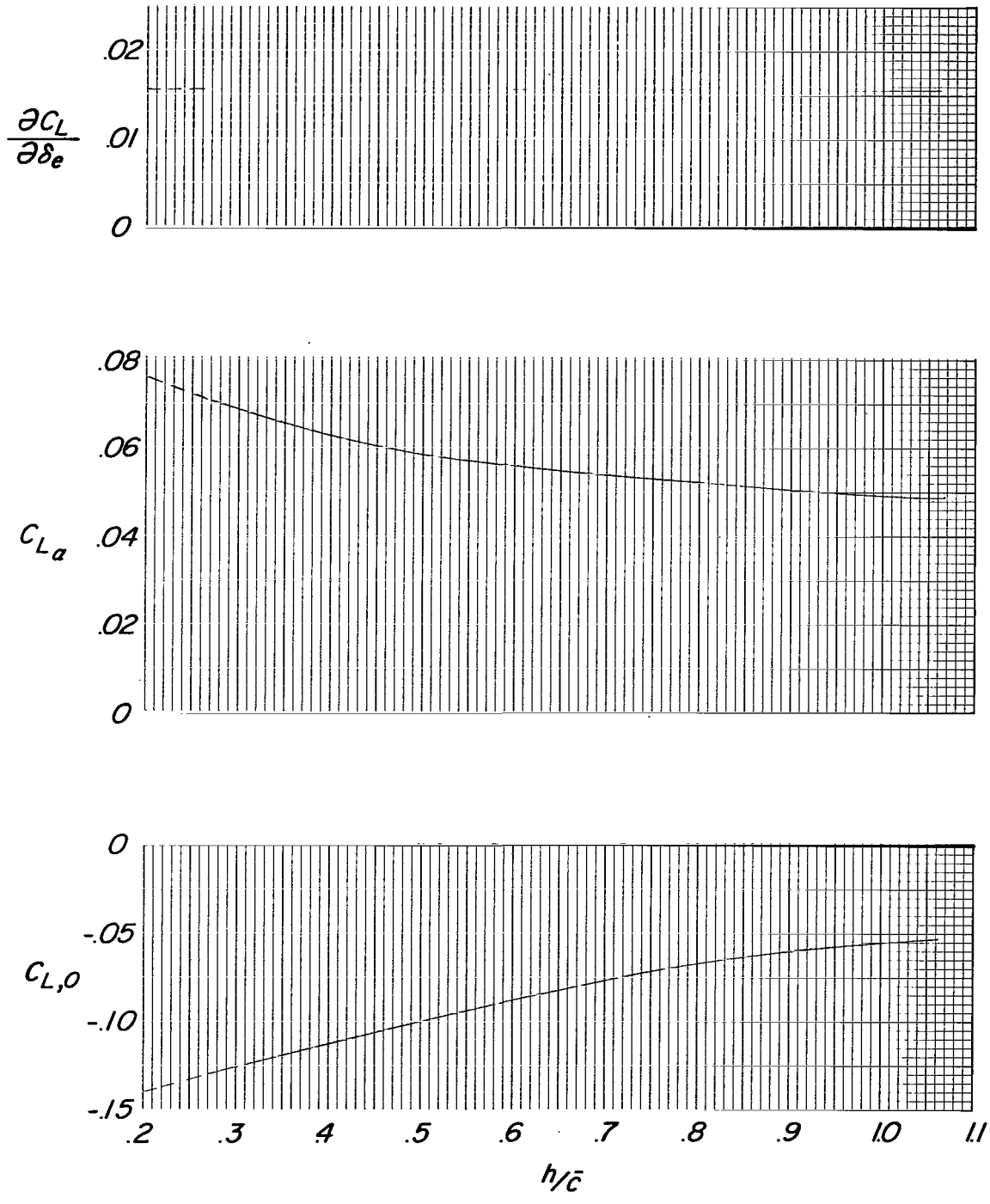

(a) Lift parameters.

Figure 8.- Variation of aerodynamic parameters used in landing-flare calculations.

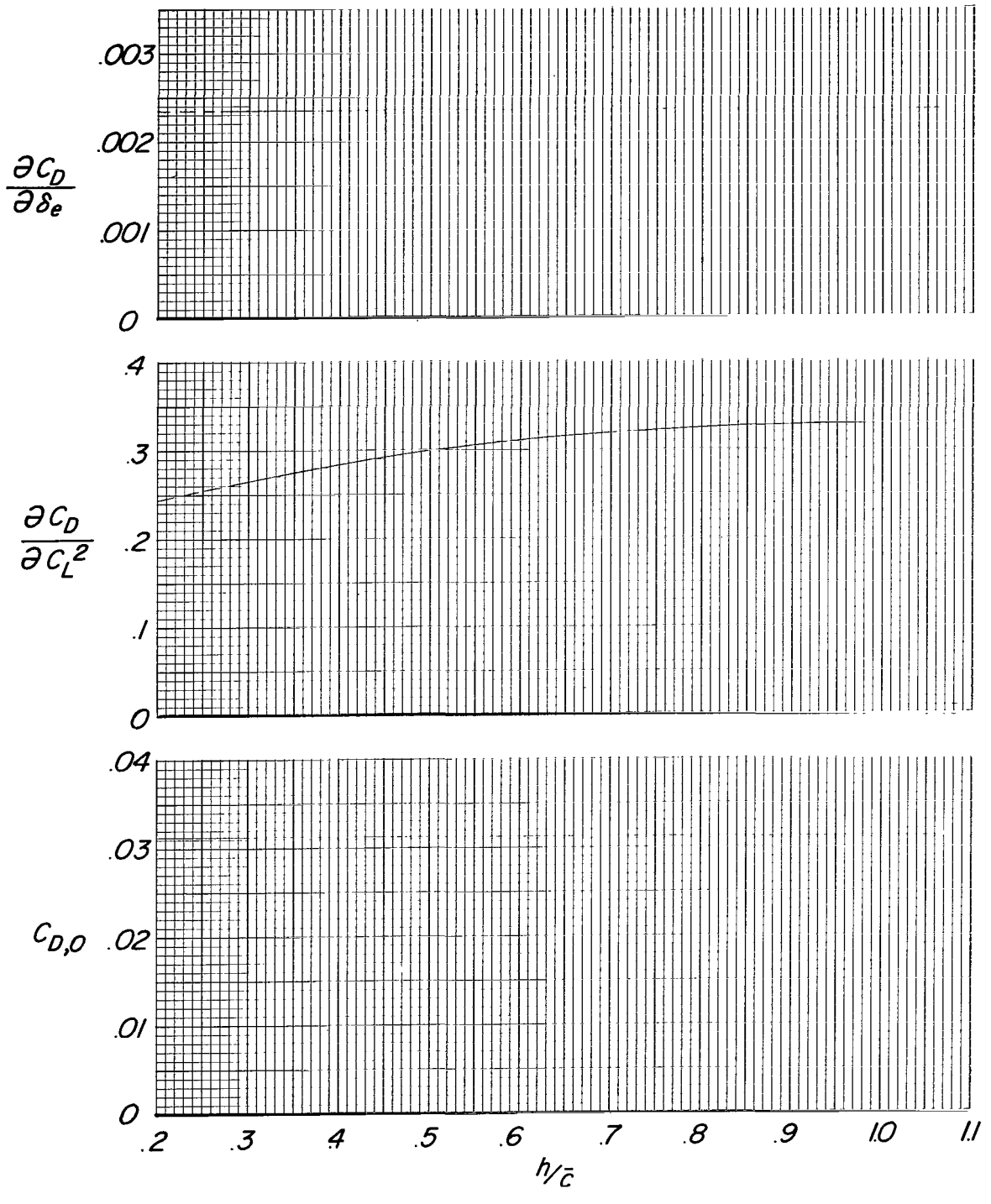

(b) Drag parameters.

Figure 8.- Continued.

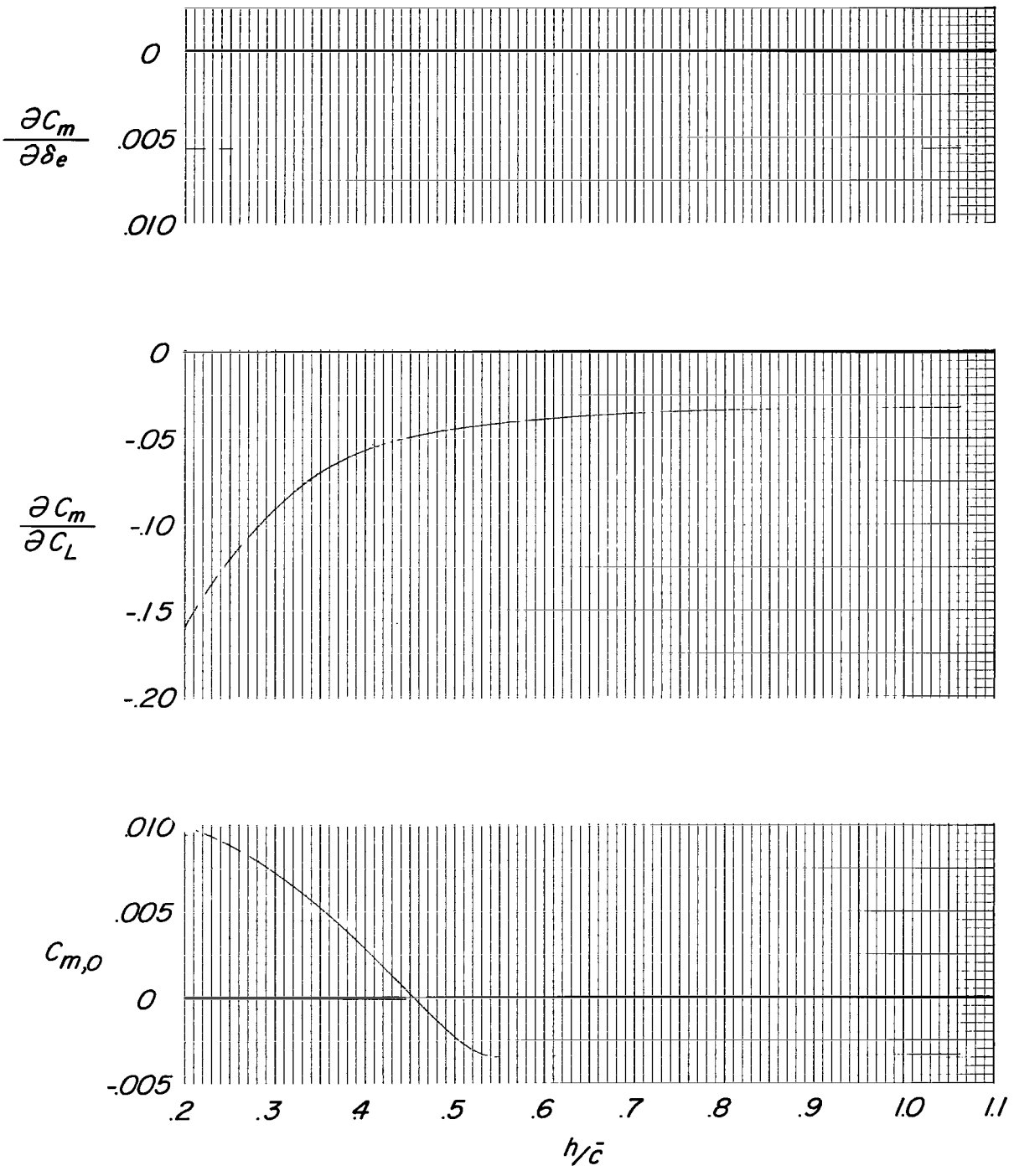

(c) Pitching-moment parameters.

Figure 8.- Concluded.

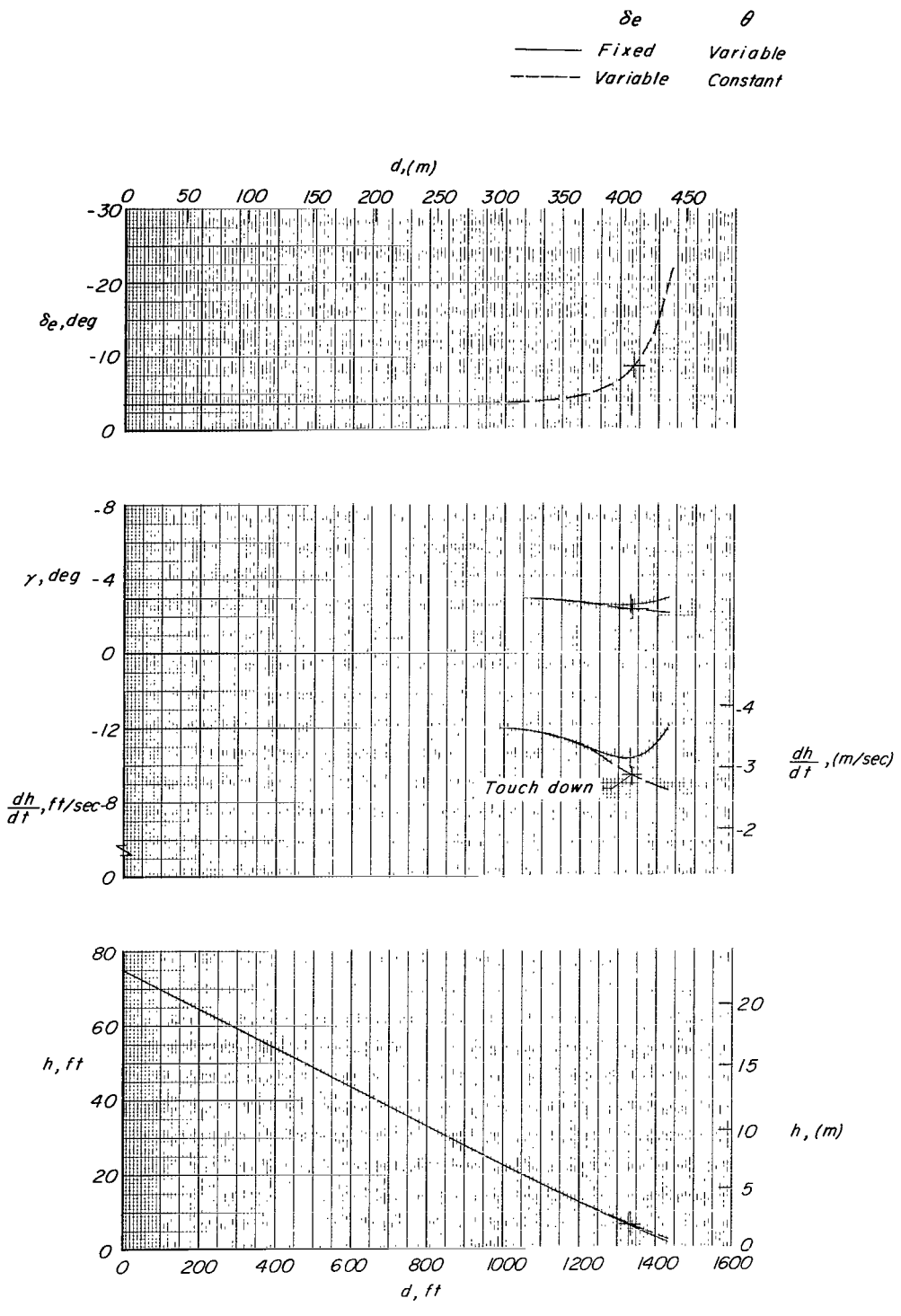

(a) Full-scale airplane. S = 661 sq ft.

Figure 9.- Calculated landing-flare maneuvers for constant attitude approaches and for fixed elevon approaches.

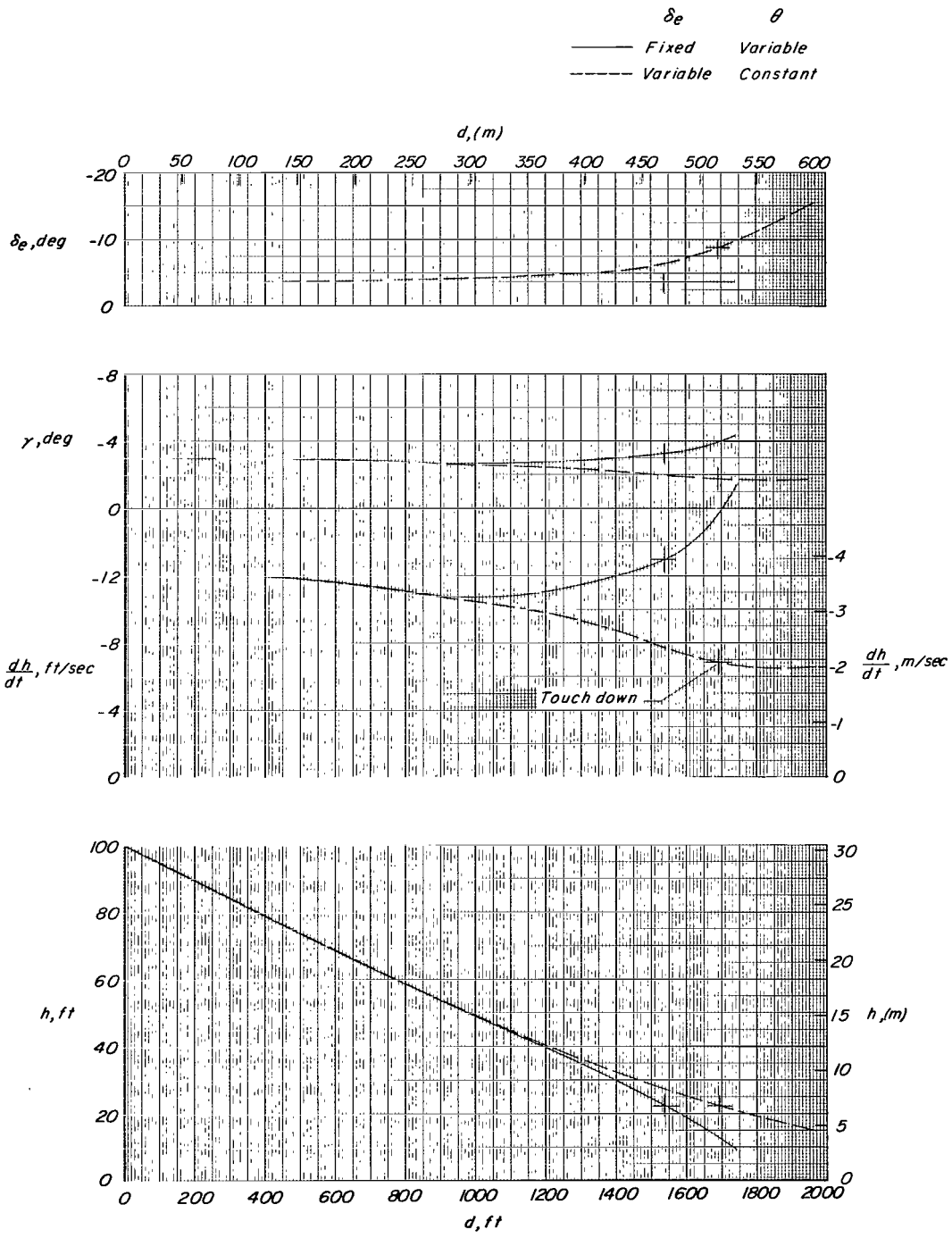

(b) Supersonic transport scale. S = 8 000 sq ft.

Figure 9.- Concluded.

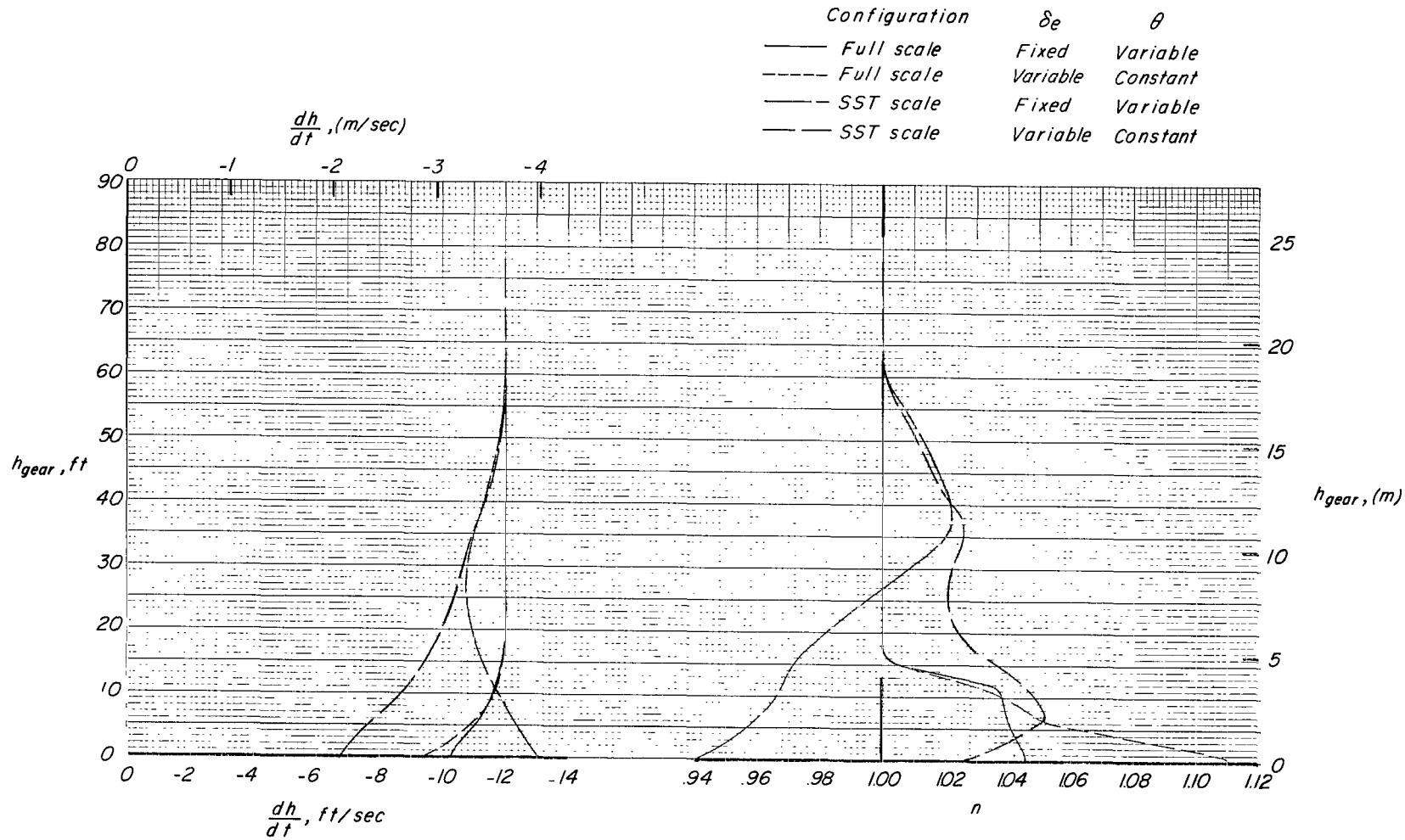

Figure 10.- Comparison of the normal load factors and rates of descent obtained in the landing-flare calculations for a full-scale fighter-type ogee-wing airplane and a version scaled to supersonic transport size.